The apical protein Apnoia interacts with Crumbs to regulate tracheal growth and inflation

PLOS Genetics

The apical protein Apnoia interacts with Crumbs to regulate tracheal growth and inflation

--Manuscript Draft--

Manuscript Number:	PGENETICS-D-18-01254R1
Full Title:	The apical protein Apnoia interacts with Crumbs to regulate tracheal growth and inflation
Short Title:	Apnoia interacts with Crumbs to regulate tracheal growth and inflation
Article Type:	Research Article
Section/Category:	General
Keywords:	airway tube; retromer; Drosophila; larva
Corresponding Author:	Elisabeth Knust Max-Planck Institute Dresden, GERMANY
Corresponding Author's Institution:	Max-Planck Institute
First Author:	Kassiani Skouloudaki
Order of Authors:	Kassiani Skouloudaki
	Dimitrios K. Papadopoulos
	Pavel Tomancak
	Elisabeth Knust
Abstract:	Most organs of multicellular organisms are built from epithelial tubes. To exert their functions, tubes rely on apico-basal polarity, on junctions, which form a barrier to separate the inside from the outside, and on a proper lumen, required for gas or liquid transport. Here we identify apnoia (apn), a novel Drosophila gene required for tracheal tube elongation and lumen stability at larval stages. Larvae lacking Apn show abnormal tracheal inflation and twisted airway tubes, but no obvious defects in early steps of tracheal maturation. apn encodes a transmembrane protein, primarily expressed in the tracheae, which exerts its function by controlling the localization of Crumbs (Crb), an evolutionarily conserved apical determinant. Apn physically interacts with Crb to control its localization and maintenance at the apical membrane of developing airways. In apn mutant tracheal cells, Crb fails to localize apically and is trapped in retromer-positive vesicles. Consistent with the role of Crb in apical membrane growth, RNAi-mediated knockdown of Crb results in decreased apical surface growth of tracheal cells and impaired axial elongation of the dorsal trunk. We conclude that Apn is a novel regulator of tracheal tube expansion in larval tracheae, the function of which is mediated by Crb.
Suggested Reviewers:	Claire Thomas Pennsylvania State University University Park : Penn State clairet@psu.edu Cell polarity, adhesion and morphogenesis in Drosophila development
	Antoine Guichet Institut Jacques Monod antoine.guichet@igm.fr Polarity and morphogenesis in Drosophila development
	Anne Uv Goteborgs Universitet anne.uv@medkem.gu.se Epithelial tubes
	Stefan Luschnig Westfalische Wilhelms-Universitat Munster luschnig@uni-muenster.de Epithelial tubes

Opposed Reviewers:	Shigeo Hayashi Riken Center for Developmental Biology Conflict of interest, works on cloesely related topics
	Ulrich Tepass University of Toronto Conflict of interest, works on cloesely related topics
	Marta Llimargas Institut of Molecular Biology Barcelona Conflict of interest, works on cloesely related topics
	Christos Samakovlis Stockholms Universitet Published with the first author while she was a postdoc with him.
Additional Information:	
Question	**Response**
Financial Disclosure Enter a financial disclosure statement that describes the sources of funding for the work included in this submission. Review the submission guidelines for detailed requirements. View published research articles from *PLOS Genetics* for specific examples. This statement is required for submission and **will appear in the published article** if the submission is accepted. Please make sure it is accurate.	The research was supported by the Max-Planck Society. The funders had no role in study design, data collection and analysis, decision to publish, or preparation of the manuscript.

Unfunded studies Enter: *The author(s) received no specific funding for this work.* **Funded studies** Enter a statement with the following details: • Initials of the authors who received each award • Grant numbers awarded to each author • The full name of each funder • URL of each funder website • Did the sponsors or funders play any role in the study design, data collection and analysis, decision to publish, or preparation of the manuscript? • **NO** - Include this sentence at the end of your statement: *The funders had no role in study design, data collection and analysis, decision to publish, or preparation of the manuscript.* • **YES** - Specify the role(s) played. * typeset	
Competing Interests Use the instructions below to enter a competing interest statement for this submission. On behalf of all authors, disclose any competing interests that could be perceived to bias this work—acknowledging all financial support and any other relevant financial or non-financial competing interests. This statement **will appear in the published article** if the submission is accepted. Please make sure it is accurate. View published research articles from *PLOS Genetics* for specific examples.	The authors have declared that no competing interests exist.

NO authors have competing interests Enter: *The authors have declared that no competing interests exist.* **Authors with competing interests** Enter competing interest details beginning with this statement: *I have read the journal's policy and the authors of this manuscript have the following competing interests: [insert competing interests here]* * typeset	
Data Availability Authors are required to make all data underlying the findings described fully available, without restriction, and from the time of publication. PLOS allows rare exceptions to address legal and ethical concerns. See the PLOS Data Policy and FAQ for detailed information. A Data Availability Statement describing where the data can be found is required at submission. Your answers to this question constitute the Data Availability Statement and will be published in the article, if accepted. **Important:** Stating 'data available on request from the author' is not sufficient. If your data are only available upon request, select 'No' for the first question and explain your exceptional situation in the text box. Do the authors confirm that all data underlying the findings described in their manuscript are fully available without restriction?	Yes - all data are fully available without restriction

Describe where the data may be found in full sentences. If you are copying our sample text, replace any instances of XXX with the appropriate details. • If the data are **held or will be held in a public repository**, include URLs, accession numbers or DOIs. If this information will only be available after acceptance, indicate this by ticking the box below. For example: *All XXX files are available from the XXX database (accession number(s) XXX, XXX.*). • If the data are all contained **within the manuscript and/or Supporting Information files**, enter the following: *All relevant data are within the manuscript and its Supporting Information files.* • If neither of these applies but you are able to provide **details of access elsewhere**, with or without limitations, please do so. For example: *Data cannot be shared publicly because of [XXX]. Data are available from the XXX Institutional Data Access / Ethics Committee (contact via XXX) for researchers who meet the criteria for access to confidential data.* *The data underlying the results presented in the study are available from (include the name of the third party and contact information or URL).* • This text is appropriate if the data are owned by a third party and authors do not have permission to share the data. * typeset	All relevant data are within the paper and its Supporting Information files
Additional data availability information:	Tick here if the URLs/accession numbers/DOIs will be available only after acceptance of the manuscript for publication so that we can ensure their inclusion before publication.

CBG
Max Planck Institute
of Molecular Cell Biology
and Genetics

PROF. DR. ELISABETH KNUST

PFOTENHAUERSTR. 108
01307 DRESDEN
Tel.: (0351) 210-1300
FAX: (0351) 210-1309
e-mail: knust@mpi-cbg.de

Dresden, 31.10.2018

Dear Editor,

we would like to submit the revised version of our manuscript entitled **"The apical protein Apnoia interacts with Crumbs to regulate tracheal growth and inflation"** for publication in PLoS Genetics.

We have addressed all points raised by the reviewers and listed them in a separate file.

We hope that you find our work interesting and are looking forward to your response.

Sincerely,

Elisabeth Knust
Kassiani Skouloudaki

Responses to reviewer's questions

Reviewer #1:

In their manuscript entitled "The apical protein Apnoia interacts with Crumbs to regulate tracheal growth and inflation," Skouloudaki, Papadopoulos and colleagues identify a novel Crumbs-interacting protein, Apnoia (Apn), which they name based on the tracheal defect observed in loss of function animals. Apn was initially identified by yeast two-hybrid as a Crumbs interactor and later shown to substantially co-localize with Crumbs in tracheal cells, although most Apn is apical as compared tot he subapical localization of Crb. A CRISPR-Cas9 generated deletion of the coding region resulted in a lethal mutation in which animals die during the second larval instar with twisted and uninflated tracheal tubes. Tube maturation was assessed and found to be defective at the stage of liquid clearance and gas-filling. Additionally, authors report that dorsal trunk tubes displayed a reduced length. Based on measurements of cells within the dorsal trunk, the authors conclude that growth along the AP axis is reduced, but not circumferential growth. In addition, the authors report that Crumbs localization is altered such that Crb is mostly within intracellular vesicles. Blocking endocytosis in an apn mutant background resulted in apical accumulation of Crbs, interrupted by the authors as indicating a requirement for Apn in Crb retention at the apical membrane, perhaps via Rab11-dependent trafficking from an endosomal compartment. The intracellular Crb in apn mutant animals was largely colocalized with the retromer component, VPS-35. The authors further report that knockdown of Crb by RNAi recapitulates the apn loss of function phenotype.

The work is interesting and appropriate for the journal. It seems largely well done, and should be considered for publication after addressing the following concerns:

• A major deficit of this manuscript is that the authors test a tracheal requirement for Crumbs and Apn by eliminating protein function in the entire animal. Crumbs, of course, is broadly expressed, and while apn expression does seem to be fairly tracheal-specific, there remains a worry that the phenotype is non-autonomous. In principle these deficits could be easily addressed.

> Since *apn* is expressed only in tracheae, its elimination in the entire animal is expected to influence only the tracheal tissue. In addition, tracheae-specific depletion of apn by RNAi exhibits the same phenotype (Suppl. Fig 3B). Finally, re-introduction of the apn cDNA in the tracheae rescues the mutant phenotype (Suppl. Fig 3C, F).

Complicating matters for Crumbs, mosaic loss of function studies in the trachea have been performed (crb11A22), and no defect reported (Schottenfeld-Roames et al., 2014). Likewise, pan-tracheal crumbs RNAi has been shown to modify the phenotype of mutants that accumulate ectopically high levels of Crumbs, but has not been shown to cause tracheal tube defects in otherwise wild type backgrounds (Song et al., 2013), at least under the RNAi conditions described. Authors should test cell autonomy or at least tracheal-specific requirements for Crb and Apn, either by eliminating them there specifically, and/or by rescuing specifically in the trachea (in the case of apn mutant larvae).

> We thank the reviewer for this important question. We have actually used different reagents from Song et al, 2013, indicated in Materials and Methods, in which we describe the crb RNAi line used by us. Indeed, previous data performed with crb[11A22] as well as with crb RNAi #

39177 did not show significant tracheal defects. In line with this, crb[11A22] and crbRNAi 39177 showed no abnormal trachea phenotype in our experiments (data not shown). Therefore we tested the crb RNAi #38373 (Hochapfel F et al., 2017, Cellular and Molecular Life Sciences), which targets the 3'UTR of the crb mRNA. We observed a trachea-specific phenotype upon knocked down, using either ubiquitously of tracheal-specific Gal4 drivers.

The same phenotypes were observed upon Apn knock-down using the aforementioned drivers. Personal communication with Michael Krahn (University of Muenster) confirmed that these authors also experienced problems with the Song et al *crb* RNAi line #39177, but not with the *crb* RNAi line #38373. Therefore we decided to perform our knockdown experiments with the line #38373 line provided by the Bloomington Stock Center.

Additional points for the authors to address include:

• Can apn mutants be rescued with transgene expression during larval stages?

New data added in Suppl. Fig 3C, F show that in approximately 20% of *apn[1]* mutant larvae gas filling (Suppl. Fig 3C) and tube length defects (Suppl. Fig 3F) are rescued upon tracheal-specific transgene expression.

• Is Crb localization in other epithelia normal in apn mutants?

New data added in Suppl. Fig 4G, H, show that Crb localization is not altered in salivary glands of stage L2 mutant in *apn[1]* larvae.

• Are tracheal defects, including Crb mislocalization, limited to multicellular tracheal tubes? or are autocellular and seamless tubes also compromised?

New data added in (Suppl. Fig 4A-B"') show that tracheal defects are not limited to multicellular tubes, but also affect autocellular and seamless tubes.

For the PLA shown in figure 1, can authors show images from more closely matched dorsal trunk segments (same metamere and same tube diameter) and provide quantitation?

We provide new data according to reviewer request in Fig. 2A-B" and Fig. 2C.

Reviewer #2:

Through a modified yeast two hybrid screen, Skouloudaki et al identify an insect-specific transmembrane protein, which they name Apnoia (Apn), as an interaction partner of the apical determinant Crumbs. Further evidence for a complex comes from co-IPs from

cultured cells and from in vivo localization data. Apn is shown to have high expression in the Drosophila tracheal system, localizing to the apical domain of tracheal cells. Generated Apn mutants display tracheal defects specifically at larval stages when tracheal remodeling events are associated with larval molting and growth. The tracheal tubes of apn mutants are abnormally short and twisted, defects associated with abnormal apical domain size and shape. These defects are also associated with a loss of Crumbs from the apical domain and abnormal accumulation of Crb in Vps35-positive vesicles. Blocking endocytosis reverses the loss of cortical Crumbs in apn mutants, and the loss of Crumbs seems to underlie the apn mutant defects since similar defects are observed following crb RNAi. This study should be of interest to cell and developmental biologists, particularly those studying insects. However, a number of points should be addressed.

1. For Figure 1H, I and J, higher magnification X-Y images of the apical surface and circumference should be shown to clarify co-localization patterns. Also, is there any degree of Apn-Crb co-localization over the apical surface to corroborate the PLA data?

> In Fig.1G-G" and H-H"(X-Y) as well as Fig.1G"' and H"' (circumference Y-Z) we provide higher magnification images that clearly show a high degree of colocalization of Apn with the other apical membrane proteins.
> In Fig.1I-I" (X-Y) and Fig.1I"' (circumference Y-Z) we provide strong evidence that Crb and Apn partially colocalize at the apical cell surface.

2. Further controls are needed for the PLA experiments. The same antibodies should be used in the experiment and control (e.g. anti-Crb plus anti-GFP or anti-Apn plus anti-GFP).

> We apologize for not making this point clear in our manuscript. We have used a *D*ECad-GFP knock-in line as well as a fosmid expressing a GFP-tagged Apn. We stained both lines with GFP and Crb antibodies. This means that the same antibodies have been used in experiment (apn-sfGFP) and control (*D*Ecad-GFP).
> We have included an additional experiment in Fig.2D-D" and Fig.2E-E", in which the same line (apn-sfGFP) was used for PLA, but different antibodies (e.g. anti-Crb plus anti-GFP (Fig.2D-D") and anti-Ecad plus anti-GFP, as control (Fig.2E-E")).

A different apical protein should be tested for a PLA signal with Crb (a different GFP-tagged protein for example) since the signal between Crb and Apn-GFP could be due to random interactions in the apical domain rather than being due to specific complexes.

> We followed the reviewer's request and we used the apical protein SAS (SAS-Venus: Stranded-at-Second fused with Venus under the tubulin promoter). We stained both lines with anti-GFP and anti-Crb. This means that the same antibodies have been used in experiment (apn-sfGFP) (Fig.2F-F") and control (SAS-Venus) (Fig.2G-G").

3. To assess whether or not Apn has Crb-independent effects on retromer function, as considered in the Discussion, or if Apn affects the trafficking of other proteins through the retromer, it would be worth testing if the Vps35 compartment enlargement in apn mutants is due to Crb or not (by examining apn mutants expressing crb RNAi).

We thank the reviewer for his/her comment that allows us to clarify this point. We have performed additional experiments, in which *crb* was down regulated by RNAi in *apn*^{1} mutants. The results show that indeed the increase in size of Vps35 positive vesicles is to some extent dependent on Crb (new Fig. 10 A-D).

4. The authors say that the apn mutant phenotypes are also seen "in larvae upon knock-down of apn by RNAi in the tracheae (Fig. 2C)". However, the label for Fig 2C indicates that the apn RNAi is driven by the ubiquitous daughterless-Gal4. RNAi of apn specifically in the tracheal system is important for demonstrating that the tracheal defects are tissue-autonomous, and that the body size and viability defects are due the tracheal defects (also the body size and viability defects should be clearly described for the tracheal RNAi of apn). An alternate approach would be to attempt rescue of the mutant phenotypes with expression of Apn specifically in the tracheal system.

Following to the reviewer's comment, we performed tracheae-specific depletion of *apn* by RNAi and observed the same gas filling and tube length defects (Suppl. Fig 3B), defects in Crb localization (Fig 5R) as well as body size reduction (Suppl. Fig 2K) as in *apn*^{1} mutant animals.

New data added in Suppl. Fig 3C, F show that in approximately 20% of *apn*^{1} mutant larvae gas filling (Suppl. Fig 3C) and tube length defects (Suppl. Fig 3F) are rescued upon tracheal-specific transgene expression.

5. Similarly, the authors say that they "knocked-down crb in tracheal tubes by expressing crb RNAi" but again the panels in Figure 8 indicate the use of da-Gal4. RNAi of crb specifically in the tracheal system is also important for the author's conclusions.

We performed tissue specific depletion of *crb* by RNAi, and observed gas filling and tube length defects (Fig 3G), similar as in *apn*^{1} mutant animals.

A typo on page 10, line 242: Suppl. Fig. S3 D-E' should be Suppl. Fig. S3 E-F.'

We have corrected the manuscript according to reviewer's request.

The apical protein Apnoia interacts with Crumbs to regulate tracheal growth and inflation

Kassiani Skouloudaki[1,*,#], Dimitrios K. Papadopoulos[1,2,#], Pavel Tomancak[1] and Elisabeth Knust[1,*]

[1]Max-Planck Institute for Molecular Cell Biology and Genetics, 01307 Dresden, Germany

*Correspondence: knust@mpi-cbg.de and skouloud@mpi-cbg.de

[#]Equal contribution

[2]present address: MRC Human Genetics Unit, MRC Institute of Genetics and Molecular Medicine at University of Edinburgh, Edinburgh, United Kingdom

Running title:
Apnoia interacts with Crumbs to regulate tracheal growth and inflation

Key Words:
airway tube, retromer, *Drosophila*, larva

Author contributions: KS, conceived the project, designed and performed the experiments, analyzed the data, prepared figures and wrote manuscript; DKP, designed and performed experiments and analyzed the data and wrote the manuscript; PT wrote the manuscript; EK initiated and supervised the project and wrote the manuscript; all authors critically reviewed the manuscript and approved it for submission.

Abstract

Most organs of multicellular organisms are built from epithelial tubes. To exert their functions, tubes rely on apico-basal polarity, on junctions, which form a barrier to separate the inside from the outside, and on a proper lumen, required for gas or liquid transport. Here we identify *apnoia* (*apn*), a novel *Drosophila* gene required for tracheal tube elongation and lumen stability at larval stages. Larvae lacking Apn show abnormal tracheal inflation and twisted airway tubes, but no obvious defects in early steps of tracheal maturation. *apn* encodes a transmembrane protein, primarily expressed in the tracheae, which exerts its function by controlling the localization of Crumbs (Crb), an evolutionarily conserved apical determinant. Apn physically interacts with Crb to control its localization and maintenance at the apical membrane of developing airways. In *apn* mutant tracheal cells, Crb fails to localize apically and is trapped in retromer-positive vesicles. Consistent with the role of Crb in apical membrane growth, RNAi-mediated knockdown of Crb results in decreased apical surface growth of tracheal cells and impaired axial elongation of the dorsal trunk. We conclude that Apn is a novel regulator of tracheal tube expansion in larval tracheae, the function of which is mediated by Crb.

Author summary

Tubular organs, such as the fruitfly airways, comprise essential functional pipes through which gas and liquid are transported. They consist of highly polarized epithelial cells that form a barrier between air and the larval body. However, during larval development, these tubes, though very rigid due to the

presence of cuticle, need to rapidly grow in size within short time-windows. To control their growth, cells have to regulate the apical membrane surface of the epithelial cells. In this work we have discovered a new gene called *apnoia*, which is important for tracheal growth and inflation at larval stages. We demonstrate that Apnoia is expressed in the apical membrane of tracheal epithelia cells, where it is required for apical membrane expansion. This function is mediated by regulating the proper localization and maintenance of the well-known apical determinant Crumbs. Both Apnoia and Crumbs proteins are required for expansion of the apical cell surface and, thereby, tube elongation. Such a mechanism is required to support the complex morphogenetic events that the tracheal system undergoes during development.

Introduction

Animal organs consist of epithelial tissues, which form the boundaries between internal and external environment [1-3]. During development, epithelia are instrumental to shape the various organs. Many epithelial tissues form tubular organs, such as the gut, the kidney or the pulmonary system. A fundamental feature of epithelial tubes and sheets is to keep the balance between the maintenance of structural integrity and tissue rigidity during organ growth and morphogenesis. To understand how this balance is achieved during rapid, temporally regulated developmental transitions from juvenile to adult body shapes, several studies in various animal models have focused on elucidating how cell proliferation, cell polarity, cell shape changes and trafficking contribute to the formation of tubular lumen length and

diameter [4-7]. The correct coordination of these processes is crucial for normal organ function. This is reflected in the fact that several human diseases are linked to defects in epithelial tube formation and maintenance, such as polycystic kidney disease or cystic fibrosis [8-11].

The developing tracheae of *Drosophila melanogaster,* a network of branched epithelial tubes that ensure oxygen supply to the cells of the body, has emerged as an ideal system to study cell fate determination and morphogenesis of epithelial tubes. The available genetic tools as well as the ease to image the tracheal system in the fly embryo has provided detailed insights into the developmental processes required to form tubular structures with defined functional lumens and have contributed to elucidate the interplay between tissue growth, differentiation and cell polarity [12-15].

The stereotypically branched tracheal system of *Drosophila* is set up at mid-embryogenesis. Once a continuous tubular network has formed, the tube expands to warrant increased oxygen supply to all tissues during animal growth. Tube expansion occurs by growth along the diameter and along the anterior-posterior axis. Growth is accompanied by the formation of a transient cable, comprised of a chitinous apical extracellular matrix (aECM), which fills the lumen of the tube. The generation of this cable requires the secretion of chitin and chitin-modifying enzymes. Mutations in genes affecting secretion or organization of the chitin cable result in excessively elongated tracheal tubes or tubes with irregular diameter (with constricted and swollen areas along the tube length) [15-17]. Axial growth, on the other hand, depends on the proper elongation of tracheal cells along the anterior- posterior axis. At later stages of

105 embryogenesis, the lumen becomes cleared and filled with air.

106 After hatching, the larvae undergo two molts, a process during which
107 animals rapidly shed and replace their exoskeleton with a new one, bigger in
108 size. For this, new chitinous aECM is secreted apically, thus surrounding the
109 old tube. Remodeling of this aECM permits tissue growth between larval
110 molts. The molting process is initiated by the separation of the old aECM from
111 the apical surface of the epithelial cells and the secretion of chitinases and
112 proteinases, which partially degrade the old cuticle. The remnants of the old
113 cuticle in each metamer are shed through the spiracular branches. This
114 process, called ecdysis, is followed immediately by clearance of the molting
115 fluid and air filling [18-20]. Interestingly, while the diameter of the dorsal trunk
116 only increases at each molt, tube length increases continuously throughout
117 larval life, particularly during intermolt periods [14]. Despite the importance of
118 tube expansion and elongation for larval development [18], the underlying
119 mechanisms that control tracheal growth at this stage remain poorly
120 understood.

121 A well-established regulator of apical domain size in developing
122 epithelia is Crumbs (Crb). Crb is a type I transmembrane protein, which acts
123 as an apical determinant of epithelial tissues [21]. It has a large extracellular
124 domain, a single transmembrane and a short cytoplasmic domain. Loss- and
125 gain-of-function experiments have shown that apical levels of Crb are
126 important for proper cell polarity, tissue integrity and growth. For instance,
127 absence of Crb in embryonic epithelia can result in loss of apical identity and
128 disruption of epithelial organization [22-24]. In contrast, overexpression of Crb
129 can trigger apical membrane expansion, which can lead to a disordered

epithelium, abnormal expansion of tracheal tubes and/or tissue overgrowth [21,25-33]. These results underscore the importance of Crb levels for epithelial development and homeostasis.

Several mechanisms have been uncovered that ensure proper levels of apical Crb. These include: stabilization of Crb at the membrane, mediated through interactions of its cytoplasmic domain with scaffolding proteins, e.g. Stardust (Sdt) or by homophilic interactions between Crb extracellular domains [26,34-36], regulation of Crb trafficking, including endocytosis by AP-2, Rab5 or Avalanche, membrane delivery by Rab11, recycling by the retromer and endocytic sorting by the ESCRT III component Shrub/Vps32 [29,33,37-41].

To gain further insight into the molecular mechanisms that regulate Crb and its activity during epithelial growth, we set out to identify novel interacting partners of Crb by using the yeast two-hybrid system. One of the candidates identified, CG15887, encodes a transmembrane protein, which localizes to the apical surface of tracheal tubes. We found that the CG15887 protein physically interacts with Crb. Based on the phenotype of mutations in CG15887, which is characterized by defects in tracheal growth and inflation during larval stages, we named this gene *apnoia* (*apn*). *apn* mutant animals die as second instar larvae with dorsal trunks displaying reduced axial growth and impaired apical surface area expansion, resulting in shorter tubes. This phenotype is correlated with the absence of Crb from the apical surface. RNAi knock-down of *crb* phenocopies the *apn* mutant phenotype of impaired longitudinal growth. These results identify Apn as the first regulator of tracheal

tube growth in the larvae, which acts through Crb to control tube axial tube expansion.

Results

Apnoia is an apical transmembrane protein expressed in *Drosophila* tracheae

To identify novel interactors of Crb, we searched for binding partners using a modified yeast two-hybrid screen (MBmate Y2H) [42,43] allowing bait and prey to interact at the yeast plasma membrane. The bait consisted of the most C-terminal extracellular EGF (epidermal growth factor)-like repeat, the transmembrane domain and the cytoplasmic tail of *Drosophila* Crb. One of the Crb interacting clones contained a 414bp cDNA insert representing the full-length transcript encoded by CG15887. Based on the tracheal inflation phenotype described below we named the gene *apnoia* (*apn*) (άπνοια, Greek for: lack of air).

The *apn mRNA* encodes a single protein isoform of 137 amino acids. Apn is predicted to contain a signal peptide at the amino terminus (1-23 aa) and two transmembrane domains (amino acids 50-72 and 79-101), based on the TMHMM transmembrane algorithm [44] prediction. Both the amino and carboxy terminus are located extracellularly, separated by a small intracellular loop (Suppl. Fig. S1). The PFAM algorithm (PFAM domains database 27.0) predicts that Apn contains two LPAM domains (47-56 aa and 78-90 aa), known as prokaryotic membrane lipoprotein lipid attachment site. Apn is highly conserved within the insect order (Suppl. Fig. S1) but does not appear to have a true orthologue in vertebrates.

To determine the tissue distribution and subcellular localization of *apn* mRNA and protein we performed *in situ* hybridizations and immunostainings of wild-type or transgenic animals, which either carried the *fosapn*$_{sfGFP}$, a

fosmid encoding the Apn protein C-terminally tagged with superfolded (sf) GFP [45], or a UAS-transgene encoding fluorescently-tagged Apn (UAS-*apn*$_{mCitrine}$). In addition, anti-Apn antibodies were raised in rabbits against a peptide of the N-terminal extracellular domain (aa 24-40). Expression of both *apn* mRNA (Fig. 1 A-C) and Apn protein (Fig. 1D-F and Suppl. Fig. S2A, B) was first detected in embryos at stage 13 in tracheal fusion cells. During embryonic stages 15 and 16, expression could also be detected in the dorsal and lateral trunks, in the visceral and dorsal branches and in the transverse connective branches. In the larvae, Apn is continuously expressed in the entire tracheal system (Suppl. Fig. S2C, D). As shown by antibody staining or Apn$_{mCitrine}$ fluorescence, Apn is restricted to the apical plasma membrane, where it co-localizes with the apical markers Stranded at second (Sas) (Fig. 1G-G'' and cross section in G"') and Uninflatable (Uif) (Fig. 1H-H'' and cross section in H"'). Apn co-localizes with Crb in the subapical region, a small region of the apical membrane apical to the adherens junctions (AJ) (Fig. 1I-I'' and cross section in I"').

This co-localization and the interaction in the yeast 2-hybrid system (Suppl. Fig. S2E) prompted us to further analyze the interaction between Apn and Crb in co-immunoprecipitation experiments. Full-length Apn (Apn^{FL}) expressed in S2R^{+} cells co-immunoprecipitated full-length Crb (Crb^{FL}) (Fig. 1J). *In situ* interactions between Crb and Apn were corroborated by Proximity Ligation Assays (PLA) [46] using the fosmid line (*fosapn*$_{sfGFP}$). We found that Crb and Apn-sfGFP interact in the larval tracheae (Fig. 2A-A", D-D" and C), whereas no interaction between Apn and *D*Ecad-GFP (negative control) was detected (Fig. 2B-B", E-E" and C), indicating that the observed signal was

specific for the Crb-Apn interaction. To exclude any random interactions between Crb and Apn in the apical domain we have tested a different apical protein (SAS-Venus)[47] for its interaction with Apn and found no increased PLA signal as compared to the signal between Crb and Apn (Fig. 2F-F”and G-G”).

apnoia is required for tracheal tube growth

To address possible functions of *apn* in tracheal development, we generated a knockout line by CRISPR-Cas9, in which the open reading frame of *apn* was replaced by DsRed (*apn*^{1}). No Apn protein could be detected with the anti-Apn antibody in homozygous *apn*^{1} mutant larvae and embryos (Suppl. Fig. S2B, D, F). In addition, no interaction between Crb and Apn was detected in *apn*^{1} mutant tracheae in PLA assays as compared to wild type tracheae (Suppl. Fig. S2G-G’).

apn^{1} mutant tracheae displayed wild type morphology in all embryonic stages, even in embryos derived from *apn*^{1} mutant germ line clones (Suppl. Fig. S2H). However, *apn*^{1} mutant larvae died at second instar with reduced body size and unusually twisted and uninflated tracheal tubes (compare Fig. 3A and B, Suppl. Fig. S2I, K). The phenotype is mostly manifested in the posterior tracheal metameres 9 (Tr9) and 10 (Tr10). Similar phenotypes were observed in larvae that carry *apn*^{1} in trans to Df(3R)Exel8158 (Suppl. Fig. S2J), a chromosomal deletion that includes the *apn* locus, as well as in larvae upon knock-down of *apn* by RNAi in the tracheae (Fig. 3C and Suppl. Fig. S2K and S3A, B). In addition, the length of the dorsal trunk was significantly reduced, as revealed by measurements of the posterior metamer length (Fig.

233 3E, F, H) The morphological and growth defects were rescued by one copy of
234 a fosmid containing the complete *apn* locus (fos*apn*$_{mCherry.NLS}$) (Fig. 3D, G, H),
235 whereas a cDNA of Apn expressed in the tracheae rescued the phenotype in
236 only 20% of the larvae (compare Suppl. Fig. S3A, D and C, F).

237 The uninflated tubes observed in *apn*^{1} deficient animals suggested
238 defects in tracheal maturation. In wild-type embryos as well as in each molting
239 step of larval development, tracheal maturation is characterized by distinct
240 sequential processes: i) secretion of a chitinous apical extracellular matrix
241 (aECM) into the lumen, which confers rigidity to the tube and is responsible
242 for tube expansion; ii) a pulse of endocytosis, resulting in the removal of
243 luminal proteins, and iii) liquid clearance and air filling [16,48]. Electron
244 micrographs of *apn*^{1} mutant larvae revealed a disorganized lumen with
245 “tongues” of cellular protrusions into the lumen (Suppl. Fig. S3G, H). This
246 phenotype is probably a consequence of the irregularly twisted tubes
247 (compare Fig. 3I, J) and not due to defects in cuticle organization, since the
248 two different cuticular layers, epicuticle and procuticle, were normally formed
249 and the spaced thickenings formed by the aECM (taenidia) [49] appeared
250 similar to that of wild type tubes (Fig. 3I, J and Suppl. Fig. S3G’, H’). This
251 conclusion is further supported by the normal expression of Dumpy (Dp) and
252 Piopio (Pio), two zona pellucida (ZP) domain proteins secreted into the lumen
253 [50,51] (Suppl. Fig. S3I-J’). The second maturation step, endocytosis of
254 luminal proteins, was also not impaired in *apn*^{1} mutant tubes either. Using the
255 heterologous secreted mCherry-tagged protein ANF (UAS-ANF-mCherry, a
256 rat Atrial Natriuretic Factor) [52] revealed normal secretion and endocytosis in
257 tracheal cells deficient for *apn*^{1} (compare Suppl. Fig. S3 K-L’). However, the

last maturation steps, liquid clearance and gas filling, were strongly affected in *apn*^{1} mutant tracheae (compare Fig. 3K, K' and L, L'). We could exclude leakage of the septate junctions (SJ) and hence loss of paracellular barrier as a cause of this phenotype, since Contactin (Con) and Discs Large (Dlg), two SJ components [53,54] were properly localized in the tracheae of *apn*^{1} mutants (Suppl. Fig. S3M-N').

Taken together, our data demonstrate that loss of *apn* affects late steps of tracheal tube maturation, including liquid clearance and gas filling, and impairs growth and morphology of the dorsal trunk at the second larval stage.

Apn supports apical membrane growth in larval tracheae

A striking defect observed in *apn*^{1} mutant larvae was a reduction in the length of the dorsal trunk (Fig. 3E-H). To determine the cellular basis of this phenotype we stained for *Drosophila* E-cadherin (*D*E-Cad) to visualize the cell outline. We could not detect significant differences in cell number within different metameres (data not shown). This led us to hypothesize that shortening of tracheal tubes is caused by defective apical cell surface expansion. Therefore, we measured the long and the short axes of cells (referred to as axial and circumferential length, respectively) (see Fig. 4A) as well as their cell surface area. While the circumferential cell length was not significantly different, the axial cell length of *apn*^{1} mutants was reduced in comparison to that of wild type cells (Fig. 4A, B and E, F). This difference was also reflected by a reduced aspect ratio of the two axes (axial to

circumferential length) (Fig. 4G) and the overall reduction of the apical surface area (Fig. 4C, D, H). From these results we conclude that Apn is required for anisotropic apical surface expansion and hence tracheal tube elongation.

Apnoia is required for maintenance of Crumbs on the apical membrane of tracheal cells

Regulation of apical cell surface area during axial growth of tracheal tubes has been shown to require junctional and polarity proteins as well as the apical protein Uif [55-58]. Therefore, to better understand the mechanism by which *apn* ensures apical membrane growth, we examined the subcellular distribution of junctional and polarity proteins in the tracheae of *apn*^{1} mutants. The AJ markers Armadillo (Arm), the *Drosophila* β-catenin [59] (Fig. 5A, B), Polychaetoid (Pyd), the single *Drosophila* ZO-1 orthologue [60] (Fig. 5C, D) and *D*E-Cad (Fig. 5E, F) localized similar as in wild type tracheae. *apn*^{1} mutant tracheal cells also showed normal distribution of Uif (Fig. 5G, H). These results indicate no major defects in apico-basal polarity and epithelial integrity of the tracheal tube in *apn*^{1} mutant larvae. The physical interaction between Apn and Crb motivated us to analyze the expression of Crb in *apn*^{1} mutants. In wild type tracheal cells of second instar larvae, Crb is localized in the subapical region, outlining the cell (Fig. 5I). In contrast, Crb strongly accumulated in cytoplasmic vesicles of multicellular, autocellular and seamless tubes in *apn*^{1} mutant tracheae and upon knock-down of *apn* (Fig. 5J, R and Suppl. Fig. S4A-D'). Consistent with these results, not only multicellular, but also autocellular and seamless tubes were twisted and uninflated (Suppl. Fig. S4E-F'). However, the total protein levels of Crb were

unchanged as revealed by western blotting (Suppl. Fig. S2F). To investigate whether *apn* is required for Crb apical localization only in the trachea we analyzed another epithelial tube, the salivary glands. A uniform apical localization of Crb was observed in both wild type and apn^{1} mutant salivary glands indicating a tracheae-specific role of *apn* (Fig. S4H-I').

Similar as Crb, Stardust (Sdt) (Fig. 5K, L) and Moesin (Moe) (Fig. 5M, N), whose subapical localization depends on Crb in many epithelia [61-64], are found in the same vesicular compartments as Crb. The introduction of one copy of the *apn* genomic locus (fos$apn_{mCherry.NLS}$) into the apn^{1} mutant background restored Crb membrane localization and suppressed the accumulation of Crumbs loaded vesicles (CLVs) (Fig. 5O-Q). These results indicate that Apn is required for Crb trafficking to or maintenance at the plasma membrane of tracheal cells.

In order to distinguish between these two possibilities, we blocked endocytosis in apn^{1} mutant tracheae chemically and genetically. After 2 hours incubation with dynasore, an inhibitor of Dynamin [65], Crb was mostly localized at the plasma membrane in apn^{1} mutant tracheal cells (Fig. 6A). In contrast, apn^{1} mutant cells incubated with dynasore-free medium showed only punctate staining of Crb (Fig. 6B). To corroborate this result, we blocked endocytosis by using $shibire^{ts1}$ (shi^{ts1}), a temperature sensitive allele of *shi*, which encodes Dynamin. When incubated at the restrictive temperature (34°C) $shi^{ts1};apn^{1}$ double mutant tracheae retained Crb at the apical plasma membrane (Fig. 6C), as compared to $shi^{ts1};apn^{1}$ mutant tracheae, incubated at the permissive temperature (25°C) (Fig. 6D). From these results we concluded, that Apn is required for Crb maintenance at the apical membrane.

A striking feature of the *apn*^{1} mutant phenotype is the accumulation of Crb in intracellular vesicles (Fig. 5I, P). To determine their identity, we analyzed components of the trafficking machinery, including markers for endosomes, lysosomes and retromer. No major co-localization was observed between CLVs and the early endosomal markers Rab5 (Fig. 7A-A") and Hrs (Suppl. Fig. S5A-A") or Rab11, a marker for the recycling endosome (Fig. 7B-B"). Interestingly, 25% of CLVs were also positive for the late endosomal marker Rab7 (Fig. 7C-C"). No major overlap was found between vesicular Crb and Lamp1 [66] or Arl8 [67], two markers of the lysosome (Suppl. Fig. S5B-B" and C-C"). Strikingly, about 79% of CLVs co-localized with the retromer component Vps35 (Fig. 8A-A").

We noticed that the majority of Vps35-positive vesicles were significantly larger in *apn*^{1} mutants, measuring around 0.7 µm (n=194 vesicles) in diameter, as compared to 0.27 µm (n=152 vesicles) in control larval tracheal cells (Fig. 8B). No significant size differences in two other trafficking compartments, such as the Arl8- (lysosomal) and the Golgin245- (*trans*-Golgi) [68] positive vesicles, were observed between the two genotypes (Fig. 8C, D). This result suggests that the size increase specifically in the Vps35-positive compartment is an aspect of the *apn*^{1} mutant phenotype.

Taken together, these results suggest that Apn maintains apical Crb by preventing its clathrin-dependent endocytosis. Loss of *apn* results in Crb accumulation in Vps35/retromer-positive vesicles of increased size.

Tracheal defects caused by *apn* depletion are mediated by *crb*

Since loss of apical Crb is often associated with reduced apical membrane [28,69,70] and Crb is depleted from the apical membrane in *apn*^{1} mutant tracheal cells, we asked whether the impaired apical surface growth observed in *apn*^{1} mutant tracheae is due to its effect on apical Crb. Since homozygous *crb* mutant embryos die with severe defects in many epithelia, including the tracheae [24,71], we knocked-down *crb* in tracheal tubes by expressing *crb* RNAi ubiquitously (using *da*-Gal4) or specifically in the tracheae (using *btl*-Gal4). This resulted in a strong depletion of Crb and its binding partner Sdt (Fig. 9A, B and A', B'), but had no effect on Apn expression and localization (Fig. 9C, D and C', D'). RNAi-mediated downregulation of *crb* reproduced several aspects of the *apn*^{1} mutant phenotypes, such as twisted tracheal tubes, lack of gas filling (Fig. 9E-H) and reduced apical surfaces of tracheal tube cells (Fig. 9I-K). No defect in apico-basal polarity was observed upon knockdown of Crb (Fig. 9I, J and I", J"). In addition, most animals died at L2 (larval stage 2) with some surviving until L3 (larval stage 3) instar larvae.

To assess whether the increased size of Vps35 positive vesicles in *apn*^{1} mutants are due to Crb accumulation in these vesicles, we knocked-down *crb* in *apn*^{1} tracheae using *btl*-Gal4. We found a small, yet significant reduction in the size of Vps35 positive vesicles in *apn*^{1} tracheal cells upon *crb* RNAi expression, compared to that of *apn*^{1} single mutants (Fig. 10A, B, D and Suppl. Fig. S6A-C). In contrast, Vps35 positive vesicles in tracheal cells expressing *crb* RNAi in otherwise wild-type animals are comparable in size to those of wild type Vps35 vesicles (compare Fig. 10C, D and Fig. 8B).

These results are the first to show that loss of *crb* results in a reduction of the apical surface area of larval tracheal cell, which in turn prevents proper tube elongation. In addition, they identify Apn as a novel regulator of apical Crb in the developing tracheae, which controls dorsal trunk maturation and expansion. Absence of *apn* leads to accumulation of Crb in Vps35 positive vesicles, which may contribute to the increase in vesicular size.

Discussion

This work identifies Apn as the first protein essential for airway maturation in *Drosophila* larval stages. Apn is expressed apically in tracheal epithelial cells, where it co-localizes and physically interacts with Crb. apn^{1} mutant larvae exhibit loss of tracheal tissue structure, manifested by tube size defects and impaired gas filling, resulting in body size reduction and lethality at second instar. At the cellular level, exclusion of Crb from the apical membrane in apn^{1} mutant larval tracheae goes along with apical cell surface reduction and an overall tracheal tube shortening. Absence of *apn* leads to Crb inhibition and accumulation in enlarged, Vps35/retromer-positive vesicles.

Elongation of the tracheal tube has been extensively studied in embryos where it has been shown to rely on different mechanisms, such as the organization of the aECM and cell shape changes [33,72-76]. Anisotropic growth of the apical plasma membrane is an additional mechanism to achieve proper longitudinal tube expansion. However, only few proteins have been described so far to regulate this process. One of these, the protein kinase Src42A, is required for the expansion of the cells in the axial direction, and loss of *Src42A* function results in tube length shortening, which is associated

406 with an increased tube diameter [72,75,77]. Src42A has been suggested to
407 exert its function, at least in part, by controlling *D*E-cadherin recycling and
408 hence adherens junctions remodeling [72] and/or by its interaction with the
409 Diaphanous-related formin *d*DAAM (*Drosophila* Dishevelled-associated
410 activator of morphogenesis), loss of which results in reduced apical levels of
411 activated pSrc42A [75]. More recently, Src42A has been suggested to control
412 axial expansion by inducing anisotropic localization of Crb along the
413 longitudinal junctions in comparison to transverse junctions [78]. However, we
414 never observed any anisotropic distribution of Crb in wild type larval tracheal
415 cells, making it unlikely that at this developmental stage, axial expansion is
416 regulated by a Src42A-dependent mechanism. This assumption is
417 corroborated by the observation that, unlike in *Src42A* mutants, the lack of
418 longitudinal expansion in *apn*^{1} mutant larval tubes is not associated with
419 circumferential expansion. Another protein regulating tube elongation in the
420 embryo is the epidermal growth factor receptor, EGFR. Expressing a
421 constitutively active EGFR results in shortened tracheal tubes with smaller
422 apical cell surfaces, but with increased diametrical growth. In this condition,
423 Crb shows altered apical distribution [78,79]. This phenotype differs from the
424 *apn*^{1} phenotype, where apical localization of Crb is almost completely lost and
425 only longitudinal tube growth is affected. This suggests that Apn executes
426 tube length expansion by a different mechanism.

427 How does decrease in tubular growth lead to loss of tracheal structure?
428 During development, the larval body, including the tracheal tissue, elongates
429 about 8-fold [18]. Impaired axial tracheal cell growth in *apn*^{1} mutants thus may
430 affect the balance between the forces exerted by the apical membrane growth

on the one hand and the resistance provided by the luminal aECM on the other, an important mechanism described previously to control tube shape in the embryo [33]. This could lead to physical rupture of tubes mutant for *apn*^{1}, allowing fluid entry. The presence of fluid would, in turn, disrupt proper gas filling, resulting in hypoxia and, consequently, in impaired body growth.

Several studies have shown that in some tissues Crb accumulation on the apical membrane is mediated by the retromer complex, which controls either the retrograde transport of Crb to the *trans*-Golgi [80] or the direct trafficking from the endosomes to the plasma membrane [39,41,79]. The physical interaction of Apn and Crb, the functional requirement of Apn for Crb apical localization and the fact that in *apn*^{1} mutants Crb is trapped in Vps35-positive/retromer vesicles all suggest that Apn is required for trafficking and/or maintenance of Crb at the apical membrane (Fig. 11).

However, the increase in the size of Vps35-positive vesicles in *apn*^{1} mutant cells, which is, to some extent, due to the accumulation of Crb, suggests defects in retromer function, which may prevent Crb lysosomal degradation. Further studies will help to elucidate at which level Apn controls Crb trafficking in larval tracheae.

Materials and Methods

Fly stocks

Flies were maintained at 25°C with 50% humidity unless stated otherwise. The fos*apn*$_{\text{sfGFP}}$ (tagging with 2XTY1-SGFP-V5-preTEV-BLRP-3XFLAGdFRT was done C-terminally) and fos*apn*$_{\text{mCherry.NLS}}$ (tagging with ubi-mCherry-NLS-T2A was done N-terminally) were provided by the Flyfos library

456 at MPI-CBG [45]. The following fly lines were used: Rab5-YFP, Rab7-YFP
457 and Rab11-YFP (http://rablibrary.mpi-cbg.de/cgi-bin/rab_overview.pl) [81]
458 (kindly provided by Marko Brankatschk), UAS-moe-GFP (kindly provided by
459 Brian Stramer) [82], UAS-ANF-mCherry (modified from [52]), and w; *D*E-
460 Cad::GFP [83], w; Sas:: Venus [47], w; btl-Gal4 [84]. The following fly stocks
461 were obtained from the Bloomington *Drosophila* Stock Center (BDSC): y[1]
462 M{w[+mC]=nos-Cas9.P}ZH-2A w[*] (BDSC, #54591), shi^{ts1} (BDSC, #7068),
463 y[1] v[1]; P{y[+t7.7] v[+t1.8]=TRiP.HMS01842}attP40 (crb^{RNAi}) (BDSC,
464 #38373), w[1118];da^{G32}-Gal4 (BDSC, #55851) [21], w[1118];
465 Df(3R)Exel8158/TM6B, Tb (BDSC, #7974) and UAS-lamp1-GFP (BDSC,
466 #42714). The CG15887 (apn^{RNAi}) (VDRC, #9070) was obtained from the
467 Vienna *Drosophila* Resource Center.
468
469 **Generation of apn^{1} mutant allele by CRISPR/Cas9**
470 Target sites were designed using the settings of the flyCRISPR
471 Optimal Target Finder (http://tools.flycrispr.molbio.wisc.edu/targetFinder/), to
472 guide Cas9 to two target sites, one at the 5'UTR (gagggtctgggccggcttacTGG)
473 and one at the 3'UTR end (gcaaagtcacggagaaatctGGG) (UPPERCASE:
474 PAM) of CG15887 (*apn*), with the aim to delete the whole Open Reading
475 Frame. The following phosphorylated DNA oligomers were used as primers
476 for PCR, using 10ng of pCFD4-U6:1U6:3tandem gRNAs as template
477 (Addgene #49411;[85]): forward primers 5'-[P]-
478 tatataggaaagatatccgggtgaacttcgGCAAAGTCACGGAGAAATCTgttttagagctaga
479 aatagcaag-3', reverse primer 5'-[P]-
480 attttaacttgctatttctagctctaaaacGTAAGCCGGCCCAGACCCTCcgacgttaaattgaa

aataggtc-3'. The resulting DNA fragment was cloned into pCFD4-U6:1U6:3tandemgRNAs via Gibson Assembly after linearization of the vector with BbsI. To replace the CG15887 ORF with 3XP3-dsRed we used the pHD-DsRed-attP vector (Addgene #51019;[86]). The homology arms necessary to obtain Homology Directed Repair were sequences covering 1kb regions of upstream and downstream of 5'UTR and 3'UTR gRNA cut sites, respectively. Cloning into the vector was obtained with AarI for the 5'-homology arm (5'-HA) and SapI for the 3'-homoly arm (3'-HA). Primer sequences are: Forward primer 5'-HA (5'-TGTACACCTGCGAATTCGCCCACACTGTTTGGCATCTGGCGGCGCTCCTCC-3'), Reverse primer 5'-HA (5'-TGTACACCTGCAGATCTACTTTCTCCGTGACTTTGCTCATAGCTCATTATGG-3'), Forward primer 3'-HA (5'-GCTAGCTCTTCGTATTACTGGGCGGCTACTTGAAATTCGGGAGCC-3'), Reverse primer 3'-HA (5'-GCTAGCTCTTCGGACCCCCAATAACATGTCCGTCCGCACTACG-3'). Homology arm sequences were amplified from the BAC genomic clone BACR05K08 (obtained from BACPAC resources center (BPRC). The two plasmids were injected in a concentration of 400ng each, into nos::Cas9 embryos [85].

Generation of transgenic flies

To generate the UAS-*apn* transgenic line, the CG15887 (*apn*) cDNA (RE53127; obtained from DGRC) was cloned into pJFRC-MUH-mCitrine[87]

by BglII-NotI using standard molecular biology techniques. Plasmid constructs were injected by BestGene.

Dynasore treatment of larval tracheae

apn^{1} mutant tracheae from second instar larvae were dissected in Grace's medium supplemented with Pep/Strep. Tissues were incubated in 60µM dynasore (Enzo Life Sciences) in Grace's medium containing Pep/Strep and 2.5% FCS at room temperature for 2hr. The dynasore was washed out and tracheae were fixed in 4% FA in Grace's medium for 30min.

Yeast-two-Hybrid screen

Part of the coding sequence of a *Drosophila melanogaster crb* cDNA (encoding aa: 2034-2189) (GenBank accession number NM_001043286.1) was PCR-amplified and cloned in pB102, in frame with the STE2 leader sequence at the N-terminus and ubiquitin (Cub) at the C-terminus of the bait which is coupled to the artificial transcription factor LexA-VP16 (STE2-Crb-Cub-LexA-VP16). The construct was checked by sequencing. Prey fragments were isolated from an MBmate screen with *Drosophila melanogaster* Crb as bait against a *Drosophila* Embryo NubG-x (D3DE_dT) library (NubG stands for the N-terminal domain of mutated ubiquitin and x for the prey fragment). Interaction pairs were tested in duplicate as two independent clones. For each interaction, several dilutions (undiluted, 10^{-1}, 10^{-2}, 10^{-3}) of the diploid yeast cells (culture normalized at 5Å~107 cells) and expressing both bait and prey constructs were spotted in selective media. The DO-2 selective medium lacking tryptophan and leucine was used to control for growth and to verify the

presence of both the bait and prey plasmids. The different dilutions were also spotted on a selective medium without tryptophan, leucine and histidine (DO-3). Six different concentrations of 3-AT, an inhibitor of the HIS3 gene product, were added to the DO-3 plates to increase stringency and reduce possible auto activation. The following 3-AT concentrations were tested: 1, 5,10, 50, 100 and 200 mM. The 1-by-1 Yeast two-hybrid assays were performed by Hybrigenics Services, S.A.S., Paris, France (http://www.hybrigenics.com)

Cell Culture and Transfection

Drosophila S2R^{+} cells were cultured at 25 °C in Schneider's *Drosophila* medium (Sigma) supplemented with 10% fetal bovine serum. p*Act5*-Gal4 together with UAS-Apn^{FL} and/or UAS-Crb^{FL} [21] (encoding full-length Apn and Crb, respectively) was transfected into S2R^{+} cells using FuGENE HD (Promega) according to the manufacturer's protocol.

Immunoprecipitation

Transfected cells were harvested after 48 h, washed with ice-cold PBS (120 mM NaCl in phosphate buffer at pH 6.7), resuspended in lysis buffer (containing 10% glycerol; 1% Triton X-100; 1.5 mM $MgCl_2$; 120 mM NaCl; 100 mM PIPES, pH 6.8; 3 mM $CaCl_2$; 1 mM PMSF and Complete^{TM}). Cells were lysed on ice for 20min and lysates were spinned at 14.000 rpm for 20min at 4ºC. The supernatant was incubated with the antibody for 2 hours. In the meantime 50µl of Protein G were washed 3 times with blocking solution and incubated with the antibody solution overnight at 4°C. Protein G beads were collected by centrifugation for 2 min at 3.000rpm and washed 4 times with

lysis buffer. Beads were resuspended in 1.5x SDS sample buffer and heated for 5min at 95°C.

Western Blot

Wild-type and *apn*^{1} mutant embryos and dissected larval tracheae were homogenized on ice using a Dounce tissue grinder in 1ml of lysis buffer containing 130mM NaCl, 50mM Tris-HCL pH=8, 0,5% Triton-X and protease inhibitor (Roche). After 30min at 4°C under rotation the homogenate was centrifuged for 20min at 14.000rpm. Sample buffer 3x SDS was added to the supernatant and boiled for 5min at 95^{o}C.

Proteins were separated by SDS-PAGE and blotted onto nitrocellulose 0.45 membrane (Amersham). After blocking in 5% BSA+TBST, the membrane was incubated overnight with rabbit anti-Apn diluted 1:1000, rat anti-Crb[88] diluted 1:1000 and mouse anti-alpha-tubulin (Sigma) diluted 1:5000 in blocking buffer. Peroxidase antibodies were used for detection.

Proximity Ligation assay (PLA)

Tracheae from *fosapn*$_{sfGFP}$ third instar larvae were dissected and fixed in ice cold 4% FA in PBS. Primary antibodies against GFP (rabbit anti-GFP 1:250; Invitrogen A11122) and Crb (rat anti-Crb 1:500 [88]) were added and incubated overnight at 4°C. The Duolink PLA Kit (Sigma Aldrich) was used to incubate the tissue with the PLA probes PLUS and MINUS at 37°C for 1 hour. Ligation of the PLA oligonucleotides and amplification were performed at 37°C for 30 min and 100min, respectively. Samples were mounted in Duolink mounting media and imaged using Zeiss LSM 880.

580

581 **Generation of Apn antiserum**

582 Polyclonal antibodies against CG15887 were raised in rabbits using the
583 KLH-conjugated synthetic peptide QQAANSSDSDSDVAESC (from the N-
584 terminal extracellular part) for immunization. Antibodies were subsequently
585 affinity-purified using the same peptide immobilized on SulfoLink Coupling Gel
586 (ThermoFisher #20401) and following recommendations by the manufacturer.
587 The work was performed by the MPI-CBG Antibody Facility.

588

589 **Immunohistochemistry**

590 Immunostainings on embryos were done as follows: embryos were
591 dechorionated in 50% bleach for 2min and fixed for 20min in
592 formaldehyde/heptane mixture. After devitellinization in methanol, embryos
593 were permeabilized in 0.1% Triton X-100/PBS except for rabbit anti-Apn
594 staining, for which embryos were permeabilized in 0.2% Saponin/ PBS. After
595 washing, embryos were incubated for 1h at RT in blocking solution [(0.5%w/v
596 BSA in PBST/S (0.1%v/v Triton X-100) or (0.2%w/v Saponin)]. Second instar
597 larvae were opened in PBS and fixed in 4% formaldehyde for 20min. After
598 washing in either 0.1% Triton X-100/PBS or 0.2% Saponin/ PBS (for anti-Apn
599 antibody staining), tracheae were dissected and incubated in blocking solution
600 for 1h at RT. Embryos and tracheae were incubated in primary antibodies
601 overnight at 4°C, washed and incubated with secondary antibody for 2h at
602 RT. Samples were mounted in Vectashield (Vector Laboratories) and imaged
603 with LSM 880 Laser Scanning Confocal Microscope (Carl Zeiss). Unless
604 otherwise indicated, images shown are z-stack projections of sections.

Images were processed with Fiji software [89]. Cell area measurements were obtained by using the Fiji Freehand selection tool.

The following primary antibodies were used: rabbit anti-Apn (1:500-1:1000) (this study), rabbit or rat anti-Crb (1:1000) [21,24,88], rabbit anti-Sdt (1:1000) [61], guinea pig anti-Cont (1:1500; gift from Manzoor Bhat), guinea pig anti-Uif (1:20; gift from Robert Ward), mouse anti-Pyd (1:1000; gift from Alan Fanning), rabbit anti-Pio (1:50; gift from Markus Affolter), guinea pig anti-HRS and anti-Vps26 (1:20 and 1:1000, respectively; gift from Hugo Bellen), rabbit anti-SAS (1:500 gift from Douglas Cavener), goat anti Golgin245 (1:200, DSHB), mouse anti-Arm (1:50, DSHB, N27A1), rabbit anti-Arl8 (1:100, DSHB), rat anti-*D*E-Cad (1:50, DSHB, DCAD2), mouse anti-Dlg (1:500, DSHB, 4F3), rabbit anti-GFP A11122 (1:250, Thermo Fischer), mouse anti-GFP (1:250, Roche), Chitin binding probe-633 (1:20; gift from Maria Leptin)[90]. The secondary antibodies Alexa Fluor 488, 568 and 633 (Molecular Probes) were used at 1:400 dilution.

RNA *in situ* hybridization

DIG-labelled RNA probes were synthesized from PCR templates amplified from for a full-length *apn* (RE53127) cDNA clone. Sequence specific primers for pFLC-I vector (BDGP resources) were: M13 (-21) 5'-TGTAAAACGACGGCCAGT-3' and M13 (REV) 5'-GGAAACAGCTATGACCATG-3'. PCR products were purified by PCR purification columns (Promega, PCR CleanUp system). *In vitro* transcription reactions were performed by mixing the PCR product with the polymerase mix, which includes T3 RNA polymerase. RNA was labelled with digoxigenin-

630 UTP (Roche Applied Science # 11277073910). Eggs were collected on apple
631 juice plates for 12h. Embryos were dechorionated in 50%bleach for 2min and
632 fixed for 20min in formaldehyde/heptane mixture. After devitellinization in
633 methanol embryos were processed for hybridization modified from [91].
634
635

Electron microscopy analysis

Larvae were fixed in 2% Glutaraldehyde in 0.1M PB buffer pH 7.2 for 20min at room temperature. Larvae were transferred in microcentrifuge tubes and fixed in 1%OsO_4/2% Glutaraldehyde and then 2% OsO_4. Further procedures were done according to the protocol described [92]. Ultrathin sections of 0.1µm were prepared and analyzed with Tecnai 12 BioTWIN (FEI Company).

Image analysis

We developed a Fiji script to quantify the co-localization of proteins of the trafficking machinery (e.g. retromer, lysosome, Golgi) with Crb-positive vesicles. Two channel images showing fluorescent Crb signal and protein X signal were imported into a script for the freely available Fiji software [89] and characterized for their overlap. The plugin was tested on Fiji current version: (Fiji is just ImageJ) ImageJ 2.0.0-rc-65/1.51w. The code of the scripts and its documentation are available on the project repository (https://git.mpi-cbg.de/bioimage-informatics/Skouloudaki_et_al_Crumbs_overlap_analysis).

Acknowledgments

We are grateful to S. Luschnig, Marko Brankatschk, Brian Stramer, the Bloomington *Drosophila* Stock Center and the Vienna *Drosophila* Resource Center for providing fly stocks. We thank the *Drosophila* Genomics Resource Center (DGRC; Indiana) and the Developmental Studies Hybridoma Bank (DSHB; Iowa) for clones and antibodies, and Manzoor Bhat, Robert Ward,

Allan Fanning, Markus Affolter, Hugo Bellen, Douglas Cavener and Maria Leptin for sharing antibodies. We are indebted to the Antibody Facility (Patrick Keller), the Light and Electron Microscopy Facility (Jan Peychl and Aurelien Dupont), the Image Analysis Facility (Benoit Lombardot) and the Scientific Computing Facility (Naharajan Lakshmanaperumal) at MPI-CBG for outstanding technical assistance. We thank members of the Knust lab for fruitful discussions. The research was supported by the Max-Planck Society.

References

1. Yeaman C, Grindstaff KK, Nelson WJ (1999) New perspectives on mechanisms involved in generating epithelial cell polarity. Physiol Rev 79: 73-98.
2. Honda H (2017) The world of epithelial sheets. Dev Growth Differ 59: 306-316.
3. Rodriguez-Boulan E, Macara IG (2014) Organization and execution of the epithelial polarity programme. Nat Rev Mol Cell Biol 15: 225-242.
4. Bernascone I, Hachimi M, Martin-Belmonte F (2017) Signaling Networks in Epithelial Tube Formation. Cold Spring Harb Perspect Biol 9.
5. Blasky AJ, Mangan A, Prekeris R (2015) Polarized protein transport and lumen formation during epithelial tissue morphogenesis. Annu Rev Cell Dev Biol 31: 575-591.
6. Iruela-Arispe ML, Beitel GJ (2013) Tubulogenesis. Development 140: 2851-2855.
7. Jewett CE, Prekeris R (2018) Insane in the apical membrane: Trafficking events mediating apicobasal epithelial polarity during tube morphogenesis. Traffic.
8. Davies JC, Alton EW, Bush A (2007) Cystic fibrosis. BMJ 335: 1255-1259.
9. Ganner A, Neumann-Haefelin E (2017) Genetic kidney diseases: Caenorhabditis elegans as model system. Cell Tissue Res 369: 105-118.
10. Harris PC, Torres VE (2009) Polycystic kidney disease. Annu Rev Med 60: 321-337.
11. Wilson PD (2011) Apico-basal polarity in polycystic kidney disease epithelia. Biochim Biophys Acta 1812: 1239-1248.
12. Lubarsky B, Krasnow MA (2003) Tube morphogenesis: making and shaping biological tubes. Cell 112: 19-28.
13. Maruyama R, Andrew DJ (2012) Drosophila as a model for epithelial tube formation. Dev Dyn 241: 119-135.
14. Beitel GJ, Krasnow MA (2000) Genetic control of epithelial tube size in the Drosophila tracheal system. Development 127: 3271-3282.

15. Zuo L, Iordanou E, Chandran RR, Jiang L (2013) Novel mechanisms of tube-size regulation revealed by the Drosophila trachea. Cell Tissue Res 354: 343-354.
16. Hayashi S, Dong B (2017) Shape and geometry control of the Drosophila tracheal tubule. Dev Growth Differ 59: 4-11.
17. Luschnig S, Uv A (2014) Luminal matrices: an inside view on organ morphogenesis. Exp Cell Res 321: 64-70.
18. Glasheen BM, Robbins RM, Piette C, Beitel GJ, Page-McCaw A (2010) A matrix metalloproteinase mediates airway remodeling in Drosophila. Dev Biol 344: 772-783.
19. Manning G, Krasnow MA (1993) Development of the Drosophila tracheal system. In: Bate M, Martinez-Arias A, editors. The Development of Drosophila: New York: Cold Spring Harbor Laboratory Press. pp. 609-685.
20. Whitten JM (1957) The Post-embryonic Development of the tracheal System in Drosophila melanogaster. J Cell Science 41: 132-150.
21. Wodarz A, Hinz U, Engelbert M, Knust E (1995) Expression of crumbs confers apical character on plasma membrane domains of ectodermal epithelia of Drosophila. Cell 82: 67-76.
22. Grawe F, Wodarz A, Lee B, Knust E, Skaer H (1996) The Drosophila genes crumbs and stardust are involved in the biogenesis of adherens junctions. Development 122: 951-959.
23. Tepass U (1996) Crumbs, a component of the apical membrane, is required for zonula adherens formation in primary epithelia of Drosophila. Dev Biol 177: 217-225.
24. Tepass U, Theres C, Knust E (1990) crumbs encodes an EGF-like protein expressed on apical membranes of Drosophila epithelial cells and required for organization of epithelia. Cell 61: 787-799.
25. de Vreede G, Schoenfeld JD, Windler SL, Morrison H, Lu H, et al. (2014) The Scribble module regulates retromer-dependent endocytic trafficking during epithelial polarization. Development 141: 2796-2802.
26. Fletcher GC, Lucas EP, Brain R, Tournier A, Thompson BJ (2012) Positive feedback and mutual antagonism combine to polarize Crumbs in the Drosophila follicle cell epithelium. Curr Biol 22: 1116-1122.
27. Klebes A, Knust E (2000) A conserved motif in Crumbs is required for E-cadherin localisation and zonula adherens formation in Drosophila. Curr Biol 10: 76-85.
28. Laprise P, Beronja S, Silva-Gagliardi NF, Pellikka M, Jensen AM, et al. (2006) The FERM protein Yurt is a negative regulatory component of the Crumbs complex that controls epithelial polarity and apical membrane size. Dev Cell 11: 363-374.
29. Lu H, Bilder D (2005) Endocytic control of epithelial polarity and proliferation in Drosophila. Nat Cell Biol 7: 1232-1239.
30. Moberg KH, Schelble S, Burdick SK, Hariharan IK (2005) Mutations in erupted, the Drosophila ortholog of mammalian tumor susceptibility gene 101, elicit non-cell-autonomous overgrowth. Dev Cell 9: 699-710.
31. Pellikka M, Tanentzapf G, Pinto M, Smith C, McGlade CJ, et al. (2002) Crumbs, the Drosophila homologue of human CRB1/RP12, is essential for photoreceptor morphogenesis. Nature 416: 143-149.

748 32. Tanentzapf G, Smith C, McGlade J, Tepass U (2000) Apical, lateral, and basal
749 polarization cues contribute to the development of the follicular
750 epithelium during Drosophila oogenesis. J Cell Biol 151: 891-904.
751 33. Dong B, Hannezo E, Hayashi S (2014) Balance between apical membrane
752 growth and luminal matrix resistance determines epithelial tubule shape.
753 Cell Rep 7: 941-950.
754 34. Letizia A, Ricardo S, Moussian B, Martin N, Llimargas M (2013) A functional
755 role of the extracellular domain of Crumbs in cell architecture and
756 apicobasal polarity. J Cell Sci 126: 2157-2163.
757 35. Zou J, Wang X, Wei X (2012) Crb apical polarity proteins maintain zebrafish
758 retinal cone mosaics via intercellular binding of their extracellular
759 domains. Dev Cell 22: 1261-1274.
760 36. Das S, Knust E (2018) A dual role of the extracellular domain of Drosophila
761 Crumbs for morphogenesis of the embryonic neuroectoderm. Biol Open 7.
762 37. Blankenship JT, Fuller MT, Zallen JA (2007) The Drosophila homolog of the
763 Exo84 exocyst subunit promotes apical epithelial identity. J Cell Sci 120:
764 3099-3110.
765 38. Lin YH, Currinn H, Pocha SM, Rothnie A, Wassmer T, et al. (2015) AP-2-
766 complex-mediated endocytosis of Drosophila Crumbs regulates polarity
767 by antagonizing Stardust. J Cell Sci 128: 4538-4549.
768 39. Pocha SM, Wassmer T, Niehage C, Hoflack B, Knust E (2011) Retromer
769 controls epithelial cell polarity by trafficking the apical determinant
770 Crumbs. Curr Biol 21: 1111-1117.
771 40. Roeth JF, Sawyer JK, Wilner DA, Peifer M (2009) Rab11 helps maintain apical
772 crumbs and adherens junctions in the Drosophila embryonic ectoderm.
773 PLoS One 4: e7634.
774 41. Zhou B, Wu Y, Lin X (2011) Retromer regulates apical-basal polarity through
775 recycling Crumbs. Dev Biol 360: 87-95.
776 42. Stagljar I, Korostensky C, Johnsson N, te Heesen S (1998) A genetic system
777 based on split-ubiquitin for the analysis of interactions between
778 membrane proteins in vivo. Proc Natl Acad Sci U S A 95: 5187-5192.
779 43. Dunkler A, Muller J, Johnsson N (2012) Detecting protein-protein interactions
780 with the Split-Ubiquitin sensor. Methods Mol Biol 786: 115-130.
781 44. Sonnhammer EL, von Heijne G, Krogh A (1998) A hidden Markov model for
782 predicting transmembrane helices in protein sequences. Proc Int Conf
783 Intell Syst Mol Biol 6: 175-182.
784 45. Sarov M, Barz C, Jambor H, Hein MY, Schmied C, et al. (2016) A genome-wide
785 resource for the analysis of protein localisation in Drosophila. Elife 5:
786 e12068.
787 46. Soderberg O, Gullberg M, Jarvius M, Ridderstrale K, Leuchowius KJ, et al.
788 (2006) Direct observation of individual endogenous protein complexes in
789 situ by proximity ligation. Nat Methods 3: 995-1000.
790 47. Firmino J, Tinevez JY, Knust E (2013) Crumbs affects protein dynamics in
791 anterior regions of the developing Drosophila embryo. PLoS One 8:
792 e58839.
793 48. Tsarouhas V, Senti KA, Jayaram SA, Tiklova K, Hemphala J, et al. (2007)
794 Sequential pulses of apical epithelial secretion and endocytosis drive
795 airway maturation in Drosophila. Dev Cell 13: 214-225.

796 49. Ozturk-Colak A, Moussian B, Araujo SJ (2016) Drosophila chitinous aECM and
797 its cellular interactions during tracheal development. Dev Dyn 245: 259-
798 267.
799 50. Jazwinska A, Ribeiro C, Affolter M (2003) Epithelial tube morphogenesis
800 during Drosophila tracheal development requires Piopio, a luminal ZP
801 protein. Nat Cell Biol 5: 895-901.
802 51. Bokel C, Prokop A, Brown NH (2005) Papillote and Piopio: Drosophila ZP-
803 domain proteins required for cell adhesion to the apical extracellular
804 matrix and microtubule organization. J Cell Sci 118: 633-642.
805 52. Rao S, Lang C, Levitan ES, Deitcher DL (2001) Visualization of neuropeptide
806 expression, transport, and exocytosis in Drosophila melanogaster. J
807 Neurobiol 49: 159-172.
808 53. Faivre-Sarrailh C, Banerjee S, Li J, Hortsch M, Laval M, et al. (2004)
809 Drosophila contactin, a homolog of vertebrate contactin, is required for
810 septate junction organization and paracellular barrier function.
811 Development 131: 4931-4942.
812 54. Woods DF, Hough C, Peel D, Callaini G, Bryant PJ (1996) Dlg protein is
813 required for junction structure, cell polarity, and proliferation control in
814 Drosophila epithelia. J Cell Biol 134: 1469-1482.
815 55. Behr M, Riedel D, Schuh R (2003) The claudin-like megatrachea is essential in
816 septate junctions for the epithelial barrier function in Drosophila. Dev Cell
817 5: 611-620.
818 56. Laplante C, Paul SM, Beitel GJ, Nilson LA (2010) Echinoid regulates tracheal
819 morphology and fusion cell fate in Drosophila. Dev Dyn 239: 2509-2519.
820 57. Wu VM, Schulte J, Hirschi A, Tepass U, Beitel GJ (2004) Sinuous is a
821 Drosophila claudin required for septate junction organization and
822 epithelial tube size control. J Cell Biol 164: 313-323.
823 58. Zhang L, Ward REt (2009) uninflatable encodes a novel ectodermal apical
824 surface protein required for tracheal inflation in Drosophila. Dev Biol 336:
825 201-212.
826 59. Peifer M, Orsulic S, Sweeton D, Wieschaus E (1993) A role for the Drosophila
827 segment polarity gene armadillo in cell adhesion and cytoskeletal
828 integrity during oogenesis. Development 118: 1191-1207.
829 60. Choi W, Jung KC, Nelson KS, Bhat MA, Beitel GJ, et al. (2011) The single
830 Drosophila ZO-1 protein Polychaetoid regulates embryonic
831 morphogenesis in coordination with Canoe/afadin and Enabled. Mol Biol
832 Cell 22: 2010-2030.
833 61. Bachmann A, Schneider M, Theilenberg E, Grawe F, Knust E (2001)
834 Drosophila Stardust is a partner of Crumbs in the control of epithelial cell
835 polarity. Nature 414: 638-643.
836 62. Medina E, Williams J, Klipfell E, Zarnescu D, Thomas G, et al. (2002) Crumbs
837 interacts with moesin and beta(Heavy)-spectrin in the apical membrane
838 skeleton of Drosophila. J Cell Biol 158: 941-951.
839 63. Hong Y, Stronach B, Perrimon N, Jan LY, Jan YN (2001) Drosophila Stardust
840 interacts with Crumbs to control polarity of epithelia but not neuroblasts.
841 Nature 414: 634-638.
842 64. Salis P, Payre F, Valenti P, Bazellieres E, Le Bivic A, et al. (2017) Crumbs,
843 Moesin and Yurt regulate junctional stability and dynamics for a proper

morphogenesis of the Drosophila pupal wing epithelium. Sci Rep 7: 16778.
65. Macia E, Ehrlich M, Massol R, Boucrot E, Brunner C, et al. (2006) Dynasore, a cell-permeable inhibitor of dynamin. Dev Cell 10: 839-850.
66. Pulipparacharuvil S, Akbar MA, Ray S, Sevrioukov EA, Haberman AS, et al. (2005) Drosophila Vps16A is required for trafficking to lysosomes and biogenesis of pigment granules. J Cell Sci 118: 3663-3673.
67. Hofmann I, Munro S (2006) An N-terminally acetylated Arf-like GTPase is localised to lysosomes and affects their motility. J Cell Sci 119: 1494-1503.
68. Riedel F, Gillingham AK, Rosa-Ferreira C, Galindo A, Munro S (2016) An antibody toolkit for the study of membrane traffic in Drosophila melanogaster. Biol Open 5: 987-992.
69. Johnson K, Grawe F, Grzeschik N, Knust E (2002) Drosophila crumbs is required to inhibit light-induced photoreceptor degeneration. Curr Biol 12: 1675-1680.
70. Spannl S, Kumichel A, Hebbar S, Kapp K, Gonzalez-Gaitan M, et al. (2017) The Crumbs_C isoform of Drosophila shows tissue- and stage-specific expression and prevents light-dependent retinal degeneration. Biol Open 6: 165-175.
71. Tepass U, Knust E (1990) Phenotypic and developmental analysis of mutations at thecrumbs locus, a gene required for the development of epithelia inDrosophila melanogaster. Roux Arch Dev Biol 199: 189-206.
72. Forster D, Luschnig S (2012) Src42A-dependent polarized cell shape changes mediate epithelial tube elongation in Drosophila. Nat Cell Biol 14: 526-534.
73. Laprise P, Paul SM, Boulanger J, Robbins RM, Beitel GJ, et al. (2010) Epithelial polarity proteins regulate Drosophila tracheal tube size in parallel to the luminal matrix pathway. Curr Biol 20: 55-61.
74. Luschnig S, Batz T, Armbruster K, Krasnow MA (2006) serpentine and vermiform encode matrix proteins with chitin binding and deacetylation domains that limit tracheal tube length in Drosophila. Curr Biol 16: 186-194.
75. Nelson KS, Khan Z, Molnar I, Mihaly J, Kaschube M, et al. (2012) Drosophila Src regulates anisotropic apical surface growth to control epithelial tube size. Nat Cell Biol 14: 518-525.
76. Wang S, Jayaram SA, Hemphala J, Senti KA, Tsarouhas V, et al. (2006) Septate-junction-dependent luminal deposition of chitin deacetylases restricts tube elongation in the Drosophila trachea. Curr Biol 16: 180-185.
77. Ochoa-Espinosa A, Baer MM, Affolter M (2012) Tubulogenesis: Src42A goes to great lengths in tube elongation. Curr Biol 22: R446-449.
78. Olivares-Castineira I, Llimargas M (2018) Anisotropic Crb accumulation, modulated by Src42A, orients epithelial tube growth in Drosophila. biorxiv 287854.
79. Olivares-Castineira I, Llimargas M (2017) EGFR controls Drosophila tracheal tube elongation by intracellular trafficking regulation. PLoS Genet 13: e1006882.
80. Wang S, Bellen HJ (2015) The retromer complex in development and disease. Development 142: 2392-2396.

892 81. Dunst S, Kazimiers T, von Zadow F, Jambor H, Sagner A, et al. (2015)
893 Endogenously tagged rab proteins: a resource to study membrane
894 trafficking in Drosophila. Dev Cell 33: 351-365.
895 82. Dutta D, Bloor JW, Ruiz-Gomez M, VijayRaghavan K, Kiehart DP (2002) Real-
896 time imaging of morphogenetic movements in Drosophila using Gal4-
897 UAS-driven expression of GFP fused to the actin-binding domain of
898 moesin. Genesis 34: 146-151.
899 83. Huang J, Huang L, Chen YJ, Austin E, Devor CE, et al. (2011) Differential
900 regulation of adherens junction dynamics during apical-basal
901 polarization. J Cell Sci 124: 4001-4013.
902 84. Shiga Y, Tanakamatakatsu M, Hayashi S (1996) A nuclear GFP beta-
903 galactosidase fusion protein as a marker for morphogenesis in living
904 Drosophila. Development Growth & Differentiation 38: 99-106.
905 85. Port F, Chen HM, Lee T, Bullock SL (2014) Optimized CRISPR/Cas tools for
906 efficient germline and somatic genome engineering in Drosophila. Proc
907 Natl Acad Sci U S A 111: E2967-2976.
908 86. Gratz SJ, Ukken FP, Rubinstein CD, Thiede G, Donohue LK, et al. (2014) Highly
909 specific and efficient CRISPR/Cas9-catalyzed homology-directed repair in
910 Drosophila. Genetics 196: 961-971.
911 87. Pfeiffer BD, Ngo TT, Hibbard KL, Murphy C, Jenett A, et al. (2010) Refinement
912 of tools for targeted gene expression in Drosophila. Genetics 186: 735-
913 755.
914 88. Richard M, Grawe F, Knust E (2006) DPATJ plays a role in retinal
915 morphogenesis and protects against light-dependent degeneration of
916 photoreceptor cells in the Drosophila eye. Dev Dyn 235: 895-907.
917 89. Schindelin J, Arganda-Carreras I, Frise E, Kaynig V, Longair M, et al. (2012)
918 Fiji: an open-source platform for biological-image analysis. Nat Methods
919 9: 676-682.
920 90. JayaNandanan N, Mathew R, Leptin M (2014) Guidance of subcellular
921 tubulogenesis by actin under the control of a synaptotagmin-like protein
922 and Moesin. Nat Commun 5: 3036.
923 91. Tomancak P, Beaton A, Weiszmann R, Kwan E, Shu S, et al. (2002) Systematic
924 determination of patterns of gene expression during Drosophila
925 embryogenesis. Genome Biol 3: RESEARCH0088.
926 92. Mishra M, Knust E (2013) Analysis of the Drosophila compound eye with
927 light and electron microscopy. Methods Mol Biol 935: 161-182.
928

929

Figure Legends

Figure 1. Apn is a small transmembrane protein detected on the apical membrane of the tracheal epithelium.

(**A-F**) Expression of *apn* as detected by whole mount *in situ* hybridization (A-C) and *fosapn*$_{sfGFP}$ expression (D-F) in lateral views of stage 13, 15, 16, 17 embryos. *apn* RNA and protein appear first in fusion cells (FC) and later in the dorsal trunk (DT), visceral branches (VB) and dorsal branches (DB). Scale bar: 50µm.

(**G-H'''**) Apn-mCitrine (green) localizes on the apical plasma membrane together with the apical markers SAS (G, G', G") and Uif (H, H', H"), as revealed by z-projections of stage 17 tracheal tubes and optical cross sections (G''' and H'''). Scale bars: (G-G'' and H-H") 10µm, (G"') 5µm, (H"') 5µm. Arrows in G''' and H''' point to protein overlap.

(I-I''') Tracheae of btl>apn-mCitrine stage 17 embryos stained with anti-Crb (magenta) and anti-GFP (green). Cross section indicates the apical localization of Apn as compared to subapical localization of Crb. Arrows in I''' point to protein overlap. Scale bars: (I-I'') 10µm, (I"') 3µm.

(J) Co-immunoprecipitation experiments from S2R^{+} cells expressing the following constructs: UAS-Crb^{FL}+UAS-Apn^{FL} or UAS-Apn^{FL}+UAS-GFP or UAS-Crb^{FL}+UAS-GFP. Crb is co-immunoprecipitated with Apn, but not with GFP (used as negative control).

Figure 2. Apnoia interacts with Crb.

(A-B") Proximity ligation assay (PLA) shows a robust increase in number of interactions between Crb and Apn (spots in magenta) in fos*apn*$_{sfGFP}$ larval tracheae (A-A") as compared to control tracheae (*D*Ecad-GFP) (B-B"). Scale bar: 20µm.

(C) Quantification of the PLA signal produced between Crb and Apn as compared to Crb and *D*Ecad.

(D-E") Proximity ligation assay (PLA) shows increased numbers of interactions between Crb and Apn (spots in magenta) in fos*apn*$_{sfGFP}$ larval tracheae (D-D") when Crb and GFP antibodies were used as compared to fos*apn*$_{sfGFP}$ larval tracheae (E-E") when *D*Ecad and GFP antibodies were used. Scale bar: 50µm.

(F-G") Proximity ligation assay (PLA) shows a robust increase in number of interactions between Crb and Apn (spots in magenta) in fos*apn*$_{sfGFP}$ larval tracheae (F-F") as compared to a control apical protein *SAS*-Venus (G-G"). Scale bar: 50µm.

Figure 3. Apn is essential for tracheal tube maturation.

(**A-D**) Brightfield images showing the tracheal tubes of second instar larvae. Rigid and gas filled tracheal tube are present in wild type (WT) larvae (A), whereas absence of *apn* causes twisted and gas deficient tubes (B). *apn* down-regulation (*apn* RNAi) recapitulates *apn*^{1} mutant tracheal defects (C). Tube morphology defects are rescued by one genomic copy of *apn* (fos.*apn*$_{mCherry.NLS}$) (D). Anterior is to the left. Scale bar: 500µm.

(**E-G**) The 9th metamer of the dorsal trunk (yellow dotted line) of *apn*^{1} mutant second instar larvae (F) is shorter than that of wild type larvae (WT) (E).

Expression of one genomic copy of *apn* (fos.*apn*$_{mCherry.NLS}$) significantly rescues the metamer elongation defects of *apn* mutant larvae (G). Anterior is to the left. Scale bar: 200 µm.

(H) Quantification of the length of the 9th metamer of second instar tracheal tubes of wild type (WT), *apn^{1}* mutants and *apn^{1}* mutants rescued with one extra *apn* copy (fos.*apn*$_{mCherry.NLS}$;*apn^{1}*). Measurements were pooled from 6 larvae.

(**I-J**) Chitin binding probe (CBP) allows the visualization of the tracheal tube structure. Note the wrinkled and twisted tube of *apn^{1}* mutants (J) as compared to that of wild type (WT) (I) larvae. Scale bar: 50µm.

(**K-L'**) Brightfield images to show dorsal trunk diameter expansion (K, L) and gas filling (K', L') of the newly formed tracheal tube of wild type (WT, K, K') and *apn^{1}* mutant (L, L') second larval instar. Yellow indicates the tracheal cells that line along the newly formed lumen (green). Note the bubble filling the newly formed lumen in wild type (WT, white arrow) (K'), which is absent in the tube of *apn^{1}* mutants (L'), which fails to fill with gas. Scale bar: 50 µm.

Figure 4. Apn is required for longitudinal elongation of tracheal cells.

(**A-D**) Tracheal tubes of wild type (WT; A, C) and *apn^{1}* mutant (B, D) second instar larvae stained with anti-*D*E-Cad. The long and short axes of the apical surfaces (A, B) are indicated by red and green arrows, respectively, and the cells by yellow rectangles (C, D). Note that the number of cells occupying identical areas in the tracheal tube is higher (~ 4 cells) in *apn^{1}* mutants (D) than in WT (~ 1 cell) (C). Scale bars: 20 µm.

(**E-H**) The median length of the long (E) axis is significantly smaller in *apn*^{1} mutant tracheal cells than in wild type (WT) cells as compared to the short axis, which is not affected (F). The median aspect ratio (long/short axis) (G) and the median apical surface area (H) are significantly smaller in *apn*^{1} mutant tracheal cells than in wild type (WT) cells. For box plot measurements, *n* values were calculated from 48 cells (WT) and 58 cells (*apn*^{1}).

Figure 5. Apn-dependent tube growth correlates with defects in localization of Crb complex components

(A-N) Projections of confocal sections of tracheal dorsal trunks of second instar larvae. *apn*^{1} mutants stained for the adherens junction proteins Arm (B), Polychaetoid (Pyd; D), *D*E-Cad (F) and for the apical protein Uif (H) do not display any significant changes compared to the respective wild type (WT) tissues (A, C, E, G). In contrast, localization of the Crb complex proteins, Crb (I, J) and Sdt (K, L), and the FERM protein, Moe (M, N) are mis-localized in *apn*^{1} mutants. Scale bars: 20 µm.

(O-R') Tracheae of second instar larvae stained for Crb (O-R) reveals strong reduction of Crb from the apical membrane and its accumulation in cytoplasmic vesicles in *apn*^{1} mutants (P) and upon tracheal knockdown of *apn* (R). Staining for chitin binding probe (CBP; O'-R') reveals twisted tracheal tube in *apn*^{1} mutants (P') and upon tracheal knockdown of *apn* (R'), though less severe. Expression of an additional copy of *apn* (fos.apn$_{mCherry.NLS}$) rescues Crb apical localization (Q) and tubular structure defects (Q'). Scale bar: 20 µm.

Figure 6. Blocking endocytosis prevents internalization of apical Crb in *apn*-mutant tracheae.

(**A, B**) *apn*^{1} mutant tracheal tubes stained for Crb, after 2 hours incubation in 60µM dynasore (A) or in the absence of dynasore (B).

(**C, D**) Tracheal tubes hemizygous for the temperature sensitive *dynamin* allele, *shibire*^{ts1} stained for Crb, after 4 hours incubation at 34°C (C) and 25°C (D, as control). Scale bars: 20 µm.

Figure 7. Crb subcellular accumulation in *apn*^{1} mutant tracheal cells. Projections of confocal sections of second instar tracheal tubes of transgenic lines expressing the respective YFP-tagged Rab protein stained for Crb (magenta) or YFP (green). (A", B", C") show magnifications of the boxed area in (A-A', B-B', C-C') respectively.

(**A**, **A'**) *apn*^{1} mutant tracheal tubes immunostained for Crb and Rab5-YFP. (A") Magnification shows vesicular Crb, most of which does not colocalize with the Rab5.

(**B**, **B'**) *apn*^{1} mutant tracheal tubes immunostained for Crb and Rab11-YFP. Magnification (B") shows vesicular Crb, most of which does not colocalize with Rab11.

(**C**, **C'**) *apn*^{1} mutant tracheal tubes immunostained for Crb and Rab7-YFP. Magnification (C") shows vesicular Crb colocalization with Rab7 of approx. 25 %. Scale bars: A, A', B, B', C, C': 20 µm and A", B", C": 5 µm.

Figure 8. Crb is localized in abnormally large, Vps35-positive vesicles in *apn[1]* mutant tracheal cells.

(**A-A”**) Projections of confocal sections of second instar tracheal tubes, stained for Crb (magenta) and Vps35 (green). (A”) shows a magnification of the boxed area in A and A’. A substantial number (approx. 79%) of Crb-positive vesicles are also positive for Vps35 in *apn[1]* mutant tracheal cells.Scale bars: A, A’: 20 µm and A”: 5 µm.

(**B-D**) Quantification of the size of Vps35-positive vesicles (B), Arl8-positive vesicles (C) and Golgin245-positive vesicles in *apn[1]* and wild type (WT) tracheal cells. Only Vps35-positive vesicles show a significant increase in size.

Figure 9. Downregulation of *crb* induces tracheal tube defects similar to those of *apn[1]* mutant tubes.

(**A-D’**) RNAi- mediated downregulation of Crb (B, B’ and D, D’) results in strong depletion of Crb (B, D) and Sdt (B’), but does not affect Apn expression (D’) in the dorsal trunk of second instar larvae. Projections of confocal sections of second instar tracheal tubes, stained for Crb (A-D), Sdt (green; A’, B’) and Apn (green; C’, D’). Nuclear staining in C’ and D’ is due to an unspecific staining of Apn antibody. Scale bars: 20 µm.

(**E-H**) Brightfield images of second instar larvae showing the tracheal tubes. Tracheal tubes are rigid and gas filled in wild type (WT) (E). Reduction of Crb using either a ubiquitous (F) or a tracheal-specific (G) Gal4 recapitulates the

characteristic *apn[1]* mutant tracheal defects (compare F, G and H), with constricted and gas-deficient tubes. Scale bars: 20 μm.

(**I-J”**) RNAi-mediated downregulation of *crb* strongly reduces Crb (compare I’ and J’), but does not affect the localization of Arm or *D*E-Cad (compare I’ with J’ and I” with J”, respectively). Scale bars: 20 μm.

(K) Quantification of the median apical surface area of *crb* RNAi tracheal cells. The surface area is significantly reduced compared to that of wild type (WT) tracheae.

Figure 10. RNAi-mediated knockdown of *crb* reduces the size of Vps35-positive vesicles in *apn[1]* mutant tracheal cells

(**A-C**) Projections of confocal sections of second instar tracheal tubes, stained for Vps35 (green). Scale bars: A-C: 20 μm.

(**D**) Quantification of the size of Vps35-positive vesicles in tracheal crb knockdown, *apn[1]* mutants and double *apn[1]*/crb knockdown tracheal cells.

Figure 11. Model to explain Apn-mediated larval tracheal tube growth.

(**A**) Top: In the wild type (WT) dorsal trunk, the apical membrane grows along the axial axis (indicated by red arrows) and pulls the apical extracellular matrix (aECM), until the aECM resistance (indicated by green arrows) balances the forces provoked by tube elongation [33]. Bottom: In wild type tracheal cells Crb (blue) is enriched at the apical membrane where it controls apical surface growth. Apn (green) in the apical membrane is responsible for Crb maintenance and therefore ensures tube elongation. Crb trafficking involves recycling by the retromer to either the trans-Golgi network (TGN; blue

vesicles) or to the plasma membrane (red vesicles), or by Rab11, or its degradation in the lysosome.

(**B**) Top: In the *apn*^{1} mutant dorsal trunk, the pulling forces of the apical membrane expansion are decreased due to decreased growth of the apical membrane (thin red arrows), whereas the forces mediated by the aECM are likely to remain unchanged, causing breakage of the tube. Bottom: In the absence of Apn, Crb is depleted from the apical surface due to increased endocytosis. Crb is trapped in enlarged, Vps35 (retromer)-positive vesicles. It fails to be recycled (as shown by the lack of colocalization with Rab11), but is also not degraded, pointing to a functional defect of the retromer.

Supporting information

Suppl. Figure 1. Amino acid sequence alignment of the protein encoded by CG15887 (*apn*).

Prank software of the homologous sequences within the insect order was used. Colored bars indicate the protein domains. SP: Signal Peptide, N'-ECD: N-terminal Extracellular Domain, TM: Transmembrane domain, ICD: Intracellular Domain, C'-ECD: C-terminal Extracellular Domain.

Suppl. Figure 2. Apn expression in the embryonic and larval tracheae.

(**A-D**) Immunostaining of embryonic (A-B') and larval (C, D) tracheae with anti-Apn antibody shows specific tracheal staining in wild type (WT) stage 17

embryos (A) and second instar (L2) larva (C). No Apn protein can be detected in *apn[1]* mutant embryos (B) and second instar (L2) larva (D). Embryos/larvae in A', B' were additionally stained for chitin binding probe (CBP) to highlight the luminal matrix. Scale bars: 20 µm.

(**E**) Yeast-two-hybrid analysis detecting interaction between the bait (Crb) and the prey (Apn). The top plate shows growth on media lacking Tryptophan and Leucine used to verify co-transformation of plasmids as well as a growth control. The bottom plate shows the same dilutions spotted on medium lacking additionally Histidine and is used to confirm the interaction between bait and prey. Column 1 is the positive control whereas columns 2,3,4 represent the negative controls (2: pB102/pP55 empty vectors, 3: pB102 empty vector/CG15887, 4: Crb/pP55 empty vector), column 5 represents the interaction between Crb-Apn. For each interaction several dilutions (undiluted, 10^{-1}, 10^{-2}, 10^{-3}) were spotted. Interactions were tested with two independent clones (A and B).

(**F**) Western blot from lysates of larval tracheae showing the expression levels of Crb and Apn in wild type (WT) and *apn[1]* mutants. Tubulin is used as loading control. The 15 kDa, Apn-positive band is absent in the *apn[1]* mutant extract. The higher molecular weight bands are unspecific.

(G, G') Proximity ligation assay (PLA) between WT and *apn[1]* mutant larval tracheae using Apn and Crb antibodies shows that the interaction is abolished in mutants lacking *apn* as compared to wild type. Scale bar: 20µm.

(**H, I**) *apn[1]* mutant embryo (H) and larva (I) derived from germline clones (M/Z; maternal/zygotic).

(H) No defects were observed in the tracheal tubes of mutant embryos. Scale bar: 100 µm.

(I) Defects appear at second larval instar with irregular and twisted tracheal tubes (I). Scale bar: 500µm

(**J**) Brightfield image of a hemizygous second instar larva transheterozygous for *apn*^{1} and a deficiency that removes *apn*. Scale bar: 500µm.

(**K**) Body size reduction in *apn*^{1} mutants and tracheal knockdown larvae as compared to wild type larvae (bottom).

Suppl. Figure 3. *apn* controls tube elongation independent of the aECM and septate junction pathway.

(A-C) Brightfield dorsal views of second instar larvae, showing the structure of tracheal tubes of wild type (WT) (A) and tracheal-specific *apn* down-regulation (btl>*apn* RNAi), which recapitulates *apn*^{1} mutant tracheal defects (B). Tube morphology defects are partially rescued by tracheal expression of Apn (*apn*^{1}; btl>Apn). Scale bar: 500µm.

(**D-F**) The 9th metamer of the dorsal trunk (yellow dotted line) of *apn*^{1} mutant second instar larvae (E) is shorter than that of wild type larvae (WT) (D). Tracheal expression of a transgene (*apn*^{1};*btl>apn*) rescues the metamer elongation defects of *apn* mutant larvae (F). Anterior is to the left. Scale bar: 200µm.

(**G-H'**) Transmission electron micrographs of cross sections through a wild type (WT; G, G') and *apn*^{1} mutant (H, H') second instar. (G, H) are axial views of the dorsal trunk (DT), G' and H' are higher magnifications to depict the

larval cuticular ECM (epi- and procuticle) and the taenidial ridges. Scale bars: (G,H) 7,5 µm, (G',H') 700 nm.

(**I-J'**) Immunostaining of larval tracheal tubes with antibodies against the apical extracellular matrix (aECM) proteins Dumpy (Dp) (I,J) and Piopio (I',J'). Scale bars: 20 µm.

(**K-L'**) Tracheal maturation of wild type (WT) (K, K') and *apn*^{1} mutant (L, L') second instar larvae. Secretion of the luminal protein ANF-Cherry (E, F) as well as its clearance from the luminal space (K', L') are comparable between wild type (WT) and *apn*^{1} mutants. Scale bars: 50 µm.

(**M-N'**) Immunostaining of wild type (WT) and *apn*^{1} mutant tracheal tubes of second instar larvae with antibodies against the septate junction proteins Contactin (Cont) (M, N) and Discs Large (Dlg) (M', N'). Scale bar: 20 µm.

Suppl. Figure 4. Distribution of Crb in tracheal branches of distinct cellular architecture and in salivary glands.

(A-B"') Confocal projections showing tracheal tubes of wild type (WT, A-A'") and *apn*^{1} mutant (B-B"') second larval instar larvae, stained with anti-Crb. Crb localization is affected in multicellular tubes (MT), lateral branches (autocellular (AT) and seamless tubes (ST) of mutant larvae. Scale bars: (A, B, A'', B'') 20 µm and (A', B', A"', B"') 10 µm.

(**C-D'**) RNAi-mediated knockdown of *apn* by *daughterless*-Gal4 (*da*-Gal4) results in accumulation of Crb-positive cytoplasmic punctae (compare C and D) and strong reduction of Apn (compare C' and D'). Nuclear Apn signal is considered to be unspecific. Scale bars: 20 µm.

(E-F') Brightfield lateral views of second instar larvae showing the structure of multicellular tubes (MT), autocellular (AT) and seamless tubes (ST) of wild type (WT, E, E') and *apn*^{1} mutants (F, F'). Scale bars: (E, F) 200 µm and (E', F') 1000 µm.

(G-H') Confocal projections showing the salivary gland of wild type (WT, G, G') and *apn*^{1} mutants (H, H') second instar larvae, stained for Crb and Dlg. Scale bars: 20 µm.

Suppl. Figure 5. Endosomal sorting components in *apn*^{1} mutants.

(**A-A"**) *apn*^{1} mutant tracheal tubes of second instar larvae immunostained for Crb (magenta) and Hrs (green). Magnification in A" shows hardly any co-localization of vesicular Crb and Hrs.

(**B-B"**) *apn*^{1} mutant tracheal tubes of second instar larvae immunostained for Crb (magenta) and Lamp1 (green). Magnification in B" shows hardly any co-localization of vesicular Crb and Lamp1.

(**C-C"**) *apn*^{1} mutant tracheal tubes of second instar larvae immunostained for Crb (magenta) and Arl8 (green). Magnification in C" shows hardly any co-localization of vesicular Crb and Arl8 staining. Scale bars: A, A', B, B', C, C': 20 µm and A", B", C": 5 µm.

Suppl. Figure 6. Expression of Crb of *apn*^{1} and *crb* depletion tracheal cells.

(A-C') RNAi-mediated downregulation of Crb (A, C) results in depletion of Crb, but does not affect Dlg expression (A', C') in the dorsal trunk of second instar larvae. In *apn*^{1} mutants, Crb is detected in cytoplasmic punctae (B),

whereas Dlg is properly localized baso-laterally in tracheal cells (B'). Projections of confocal sections of second instar tracheal tubes, stained for Crb (A-C), Dlg (green; A'-C'). Scale bars: 20 μm.

Figure 1

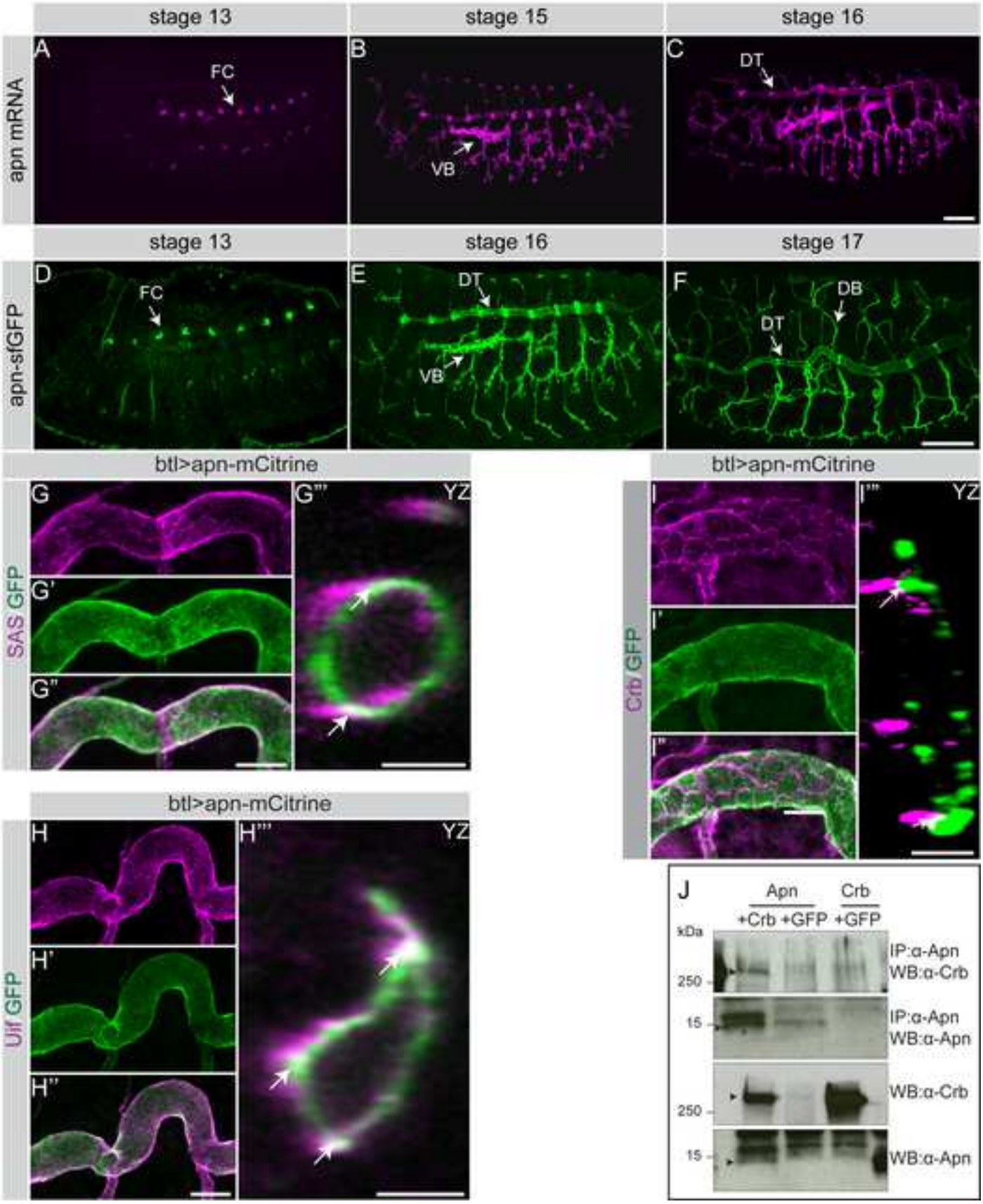

Figure 2

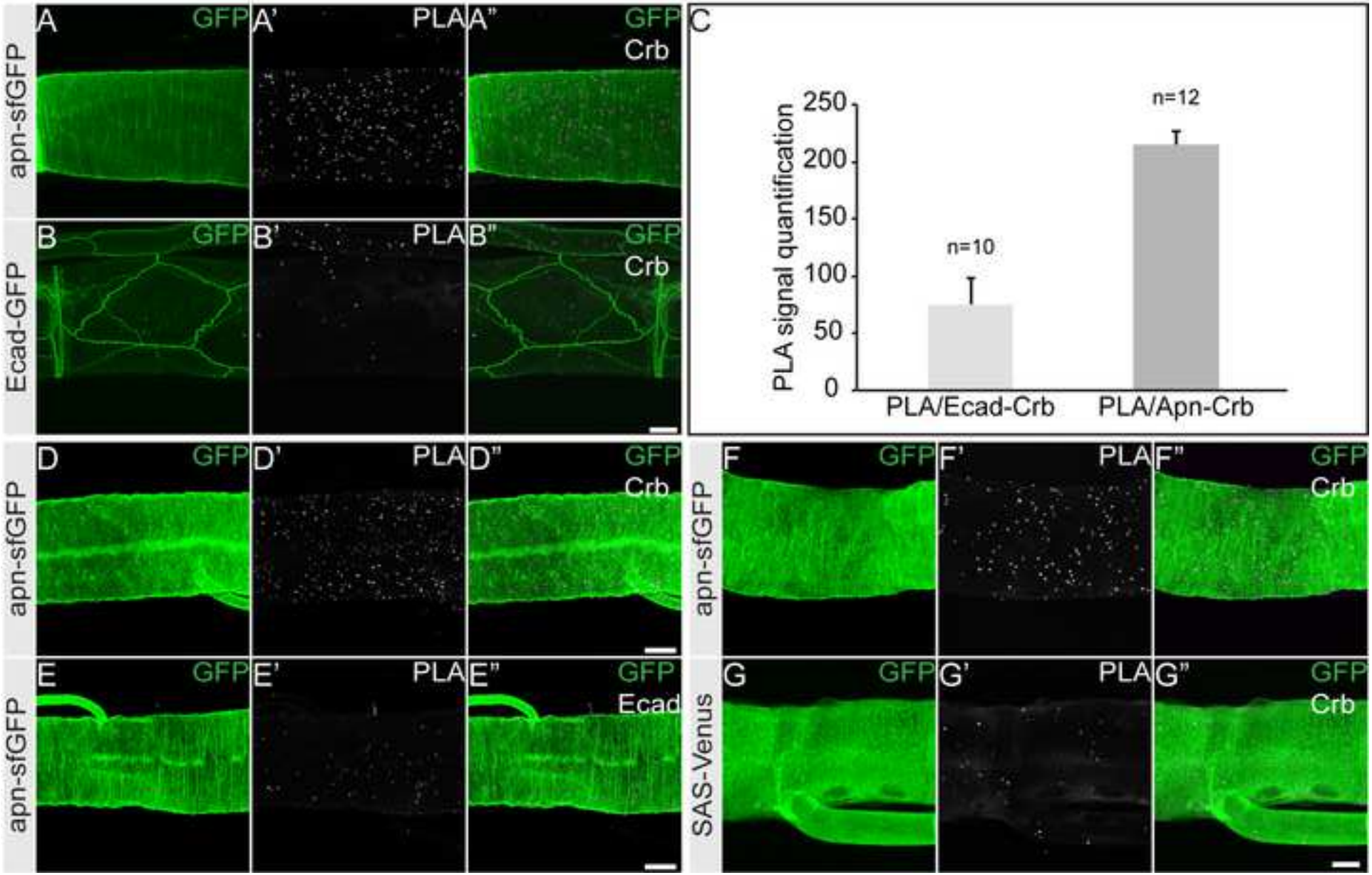

Figure 3

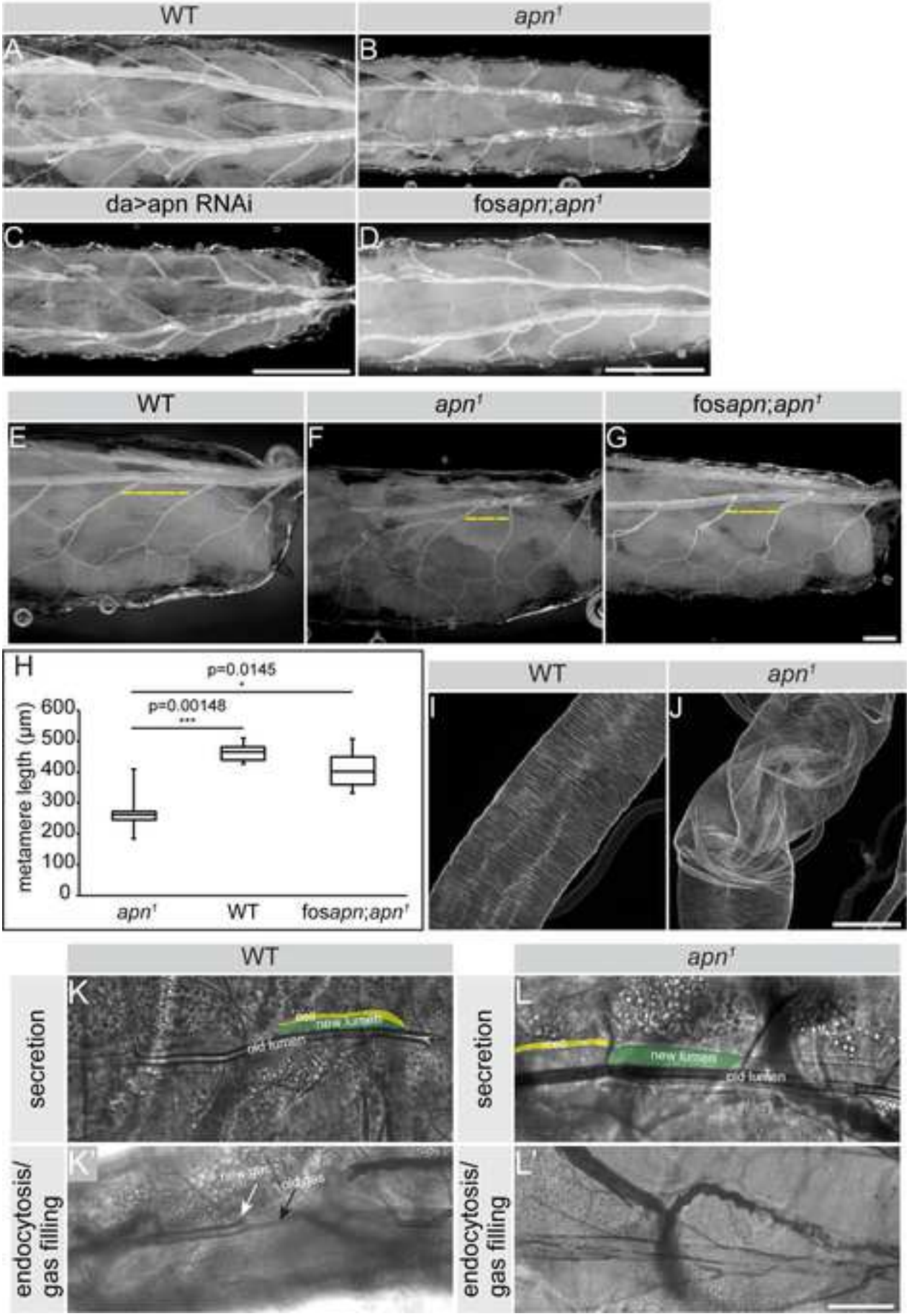

Figure 4

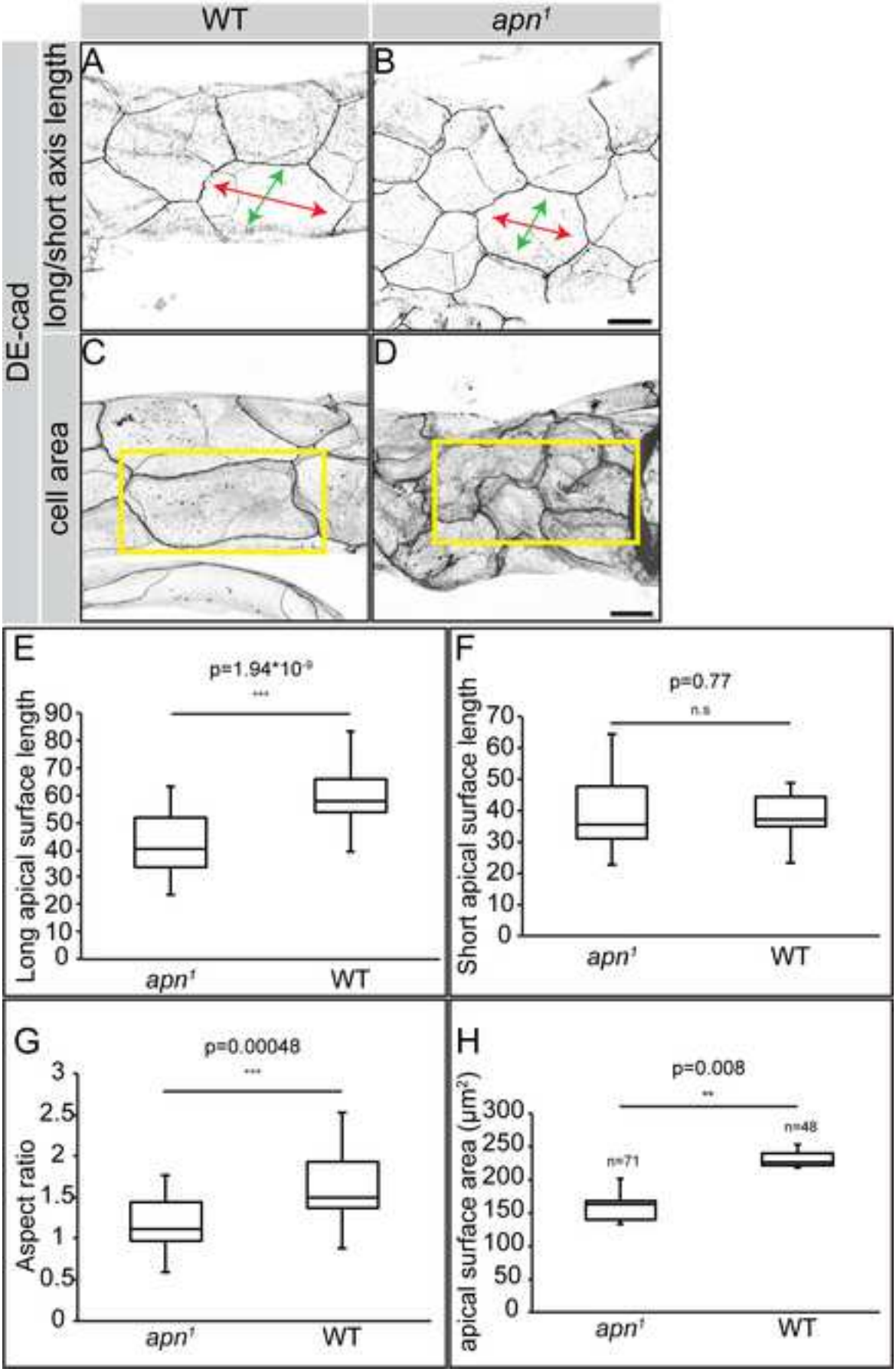

Figure 5

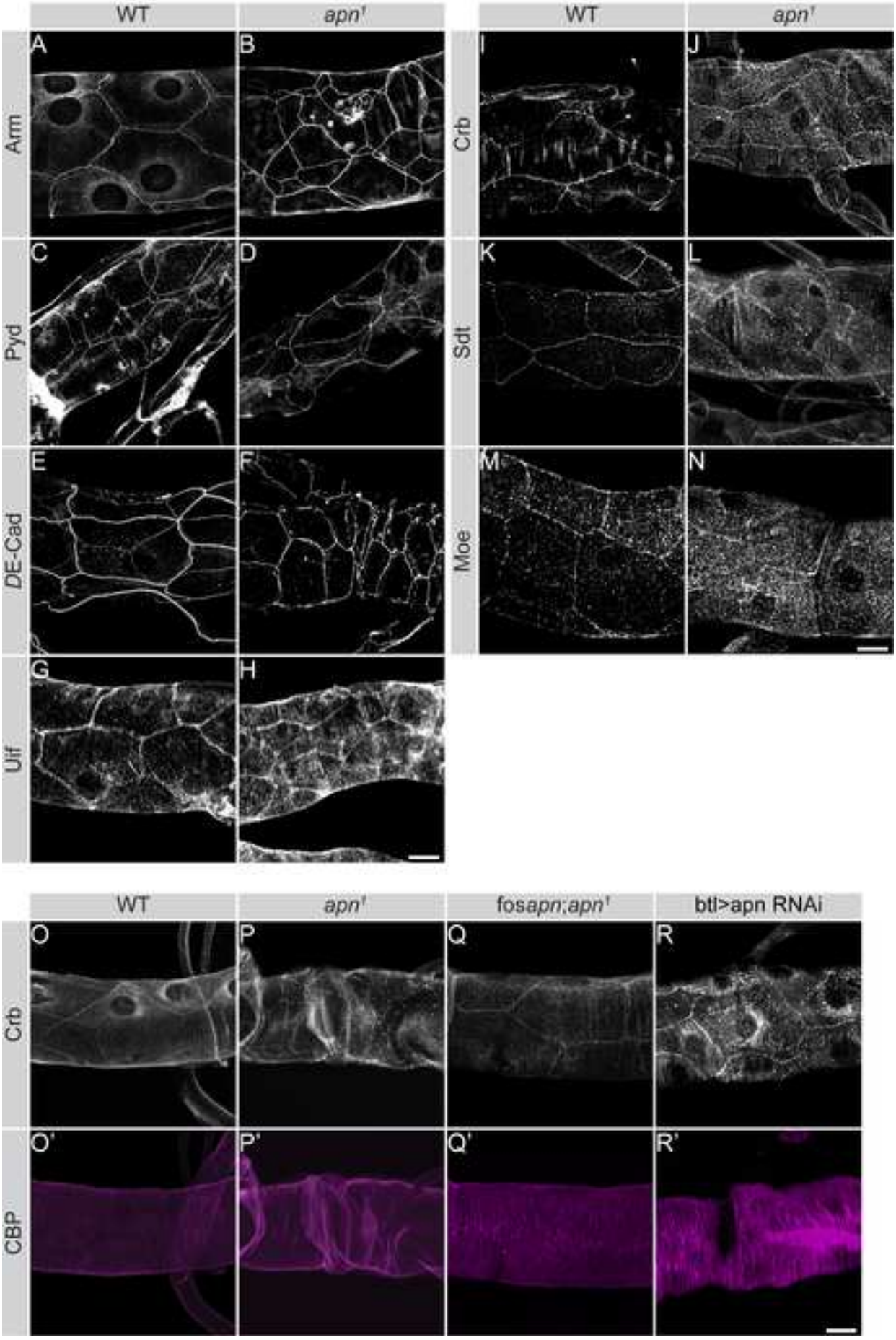

Figure 6

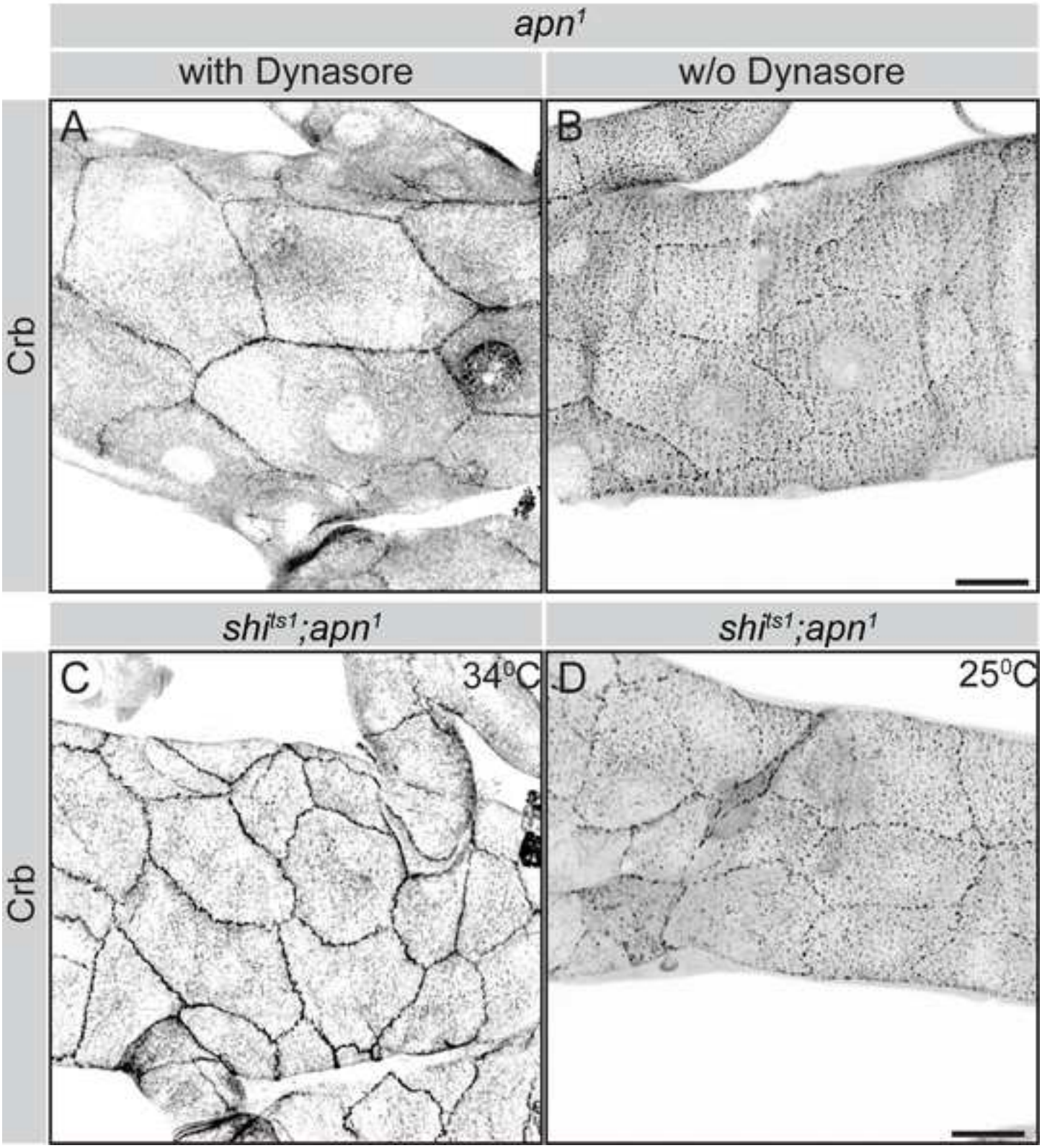

Figure 7

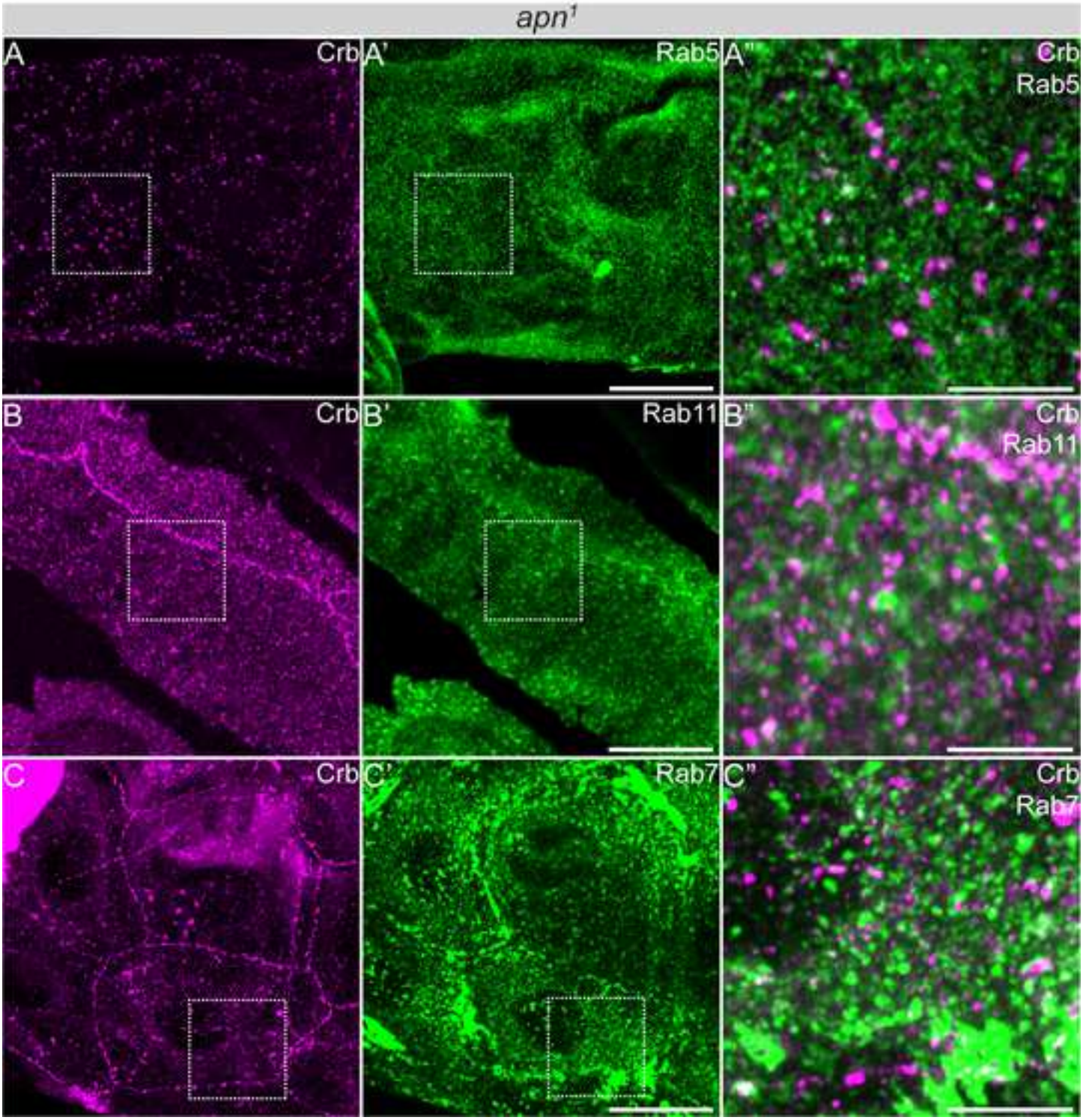

Figure 8

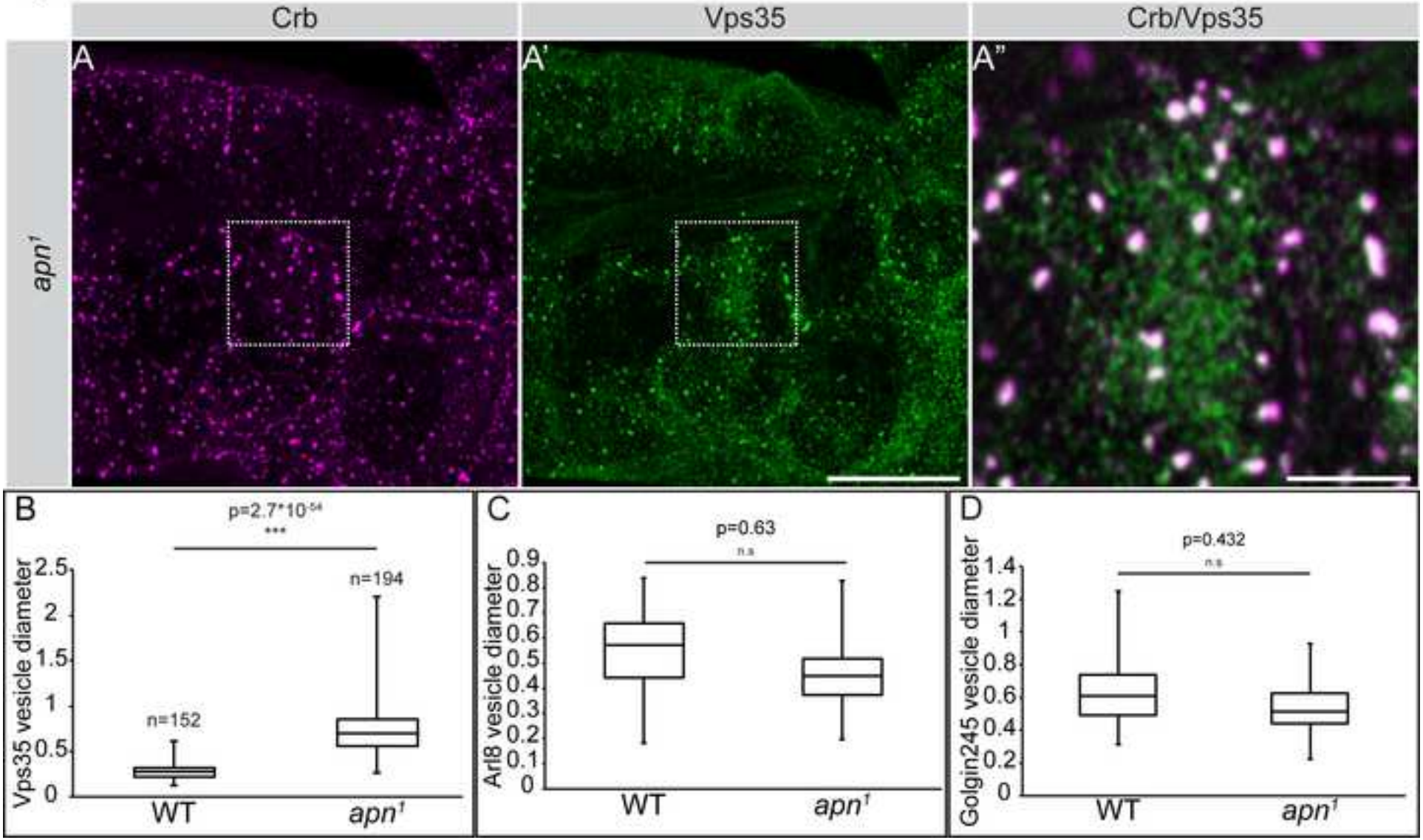

Figure 9

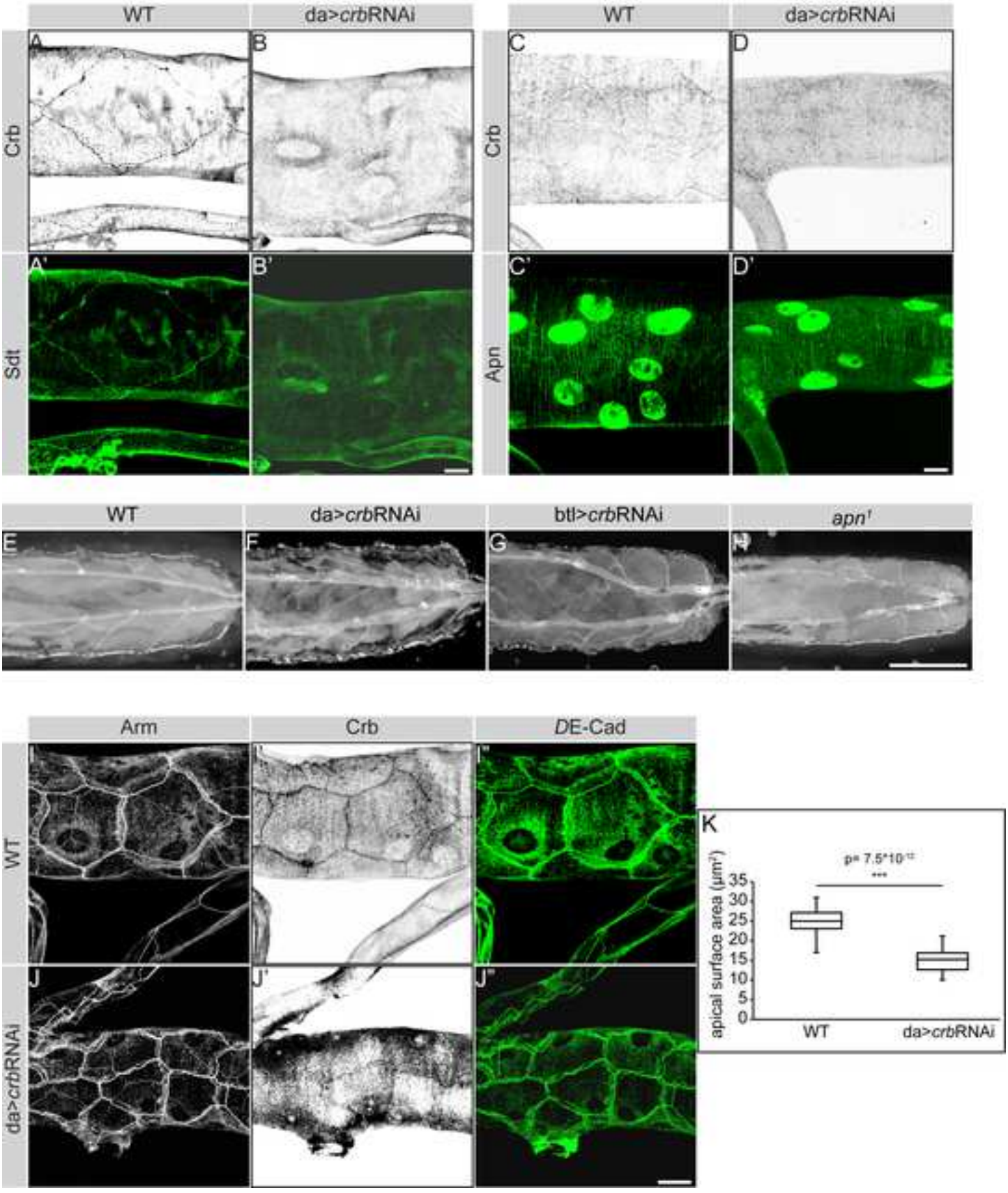

Figure 10

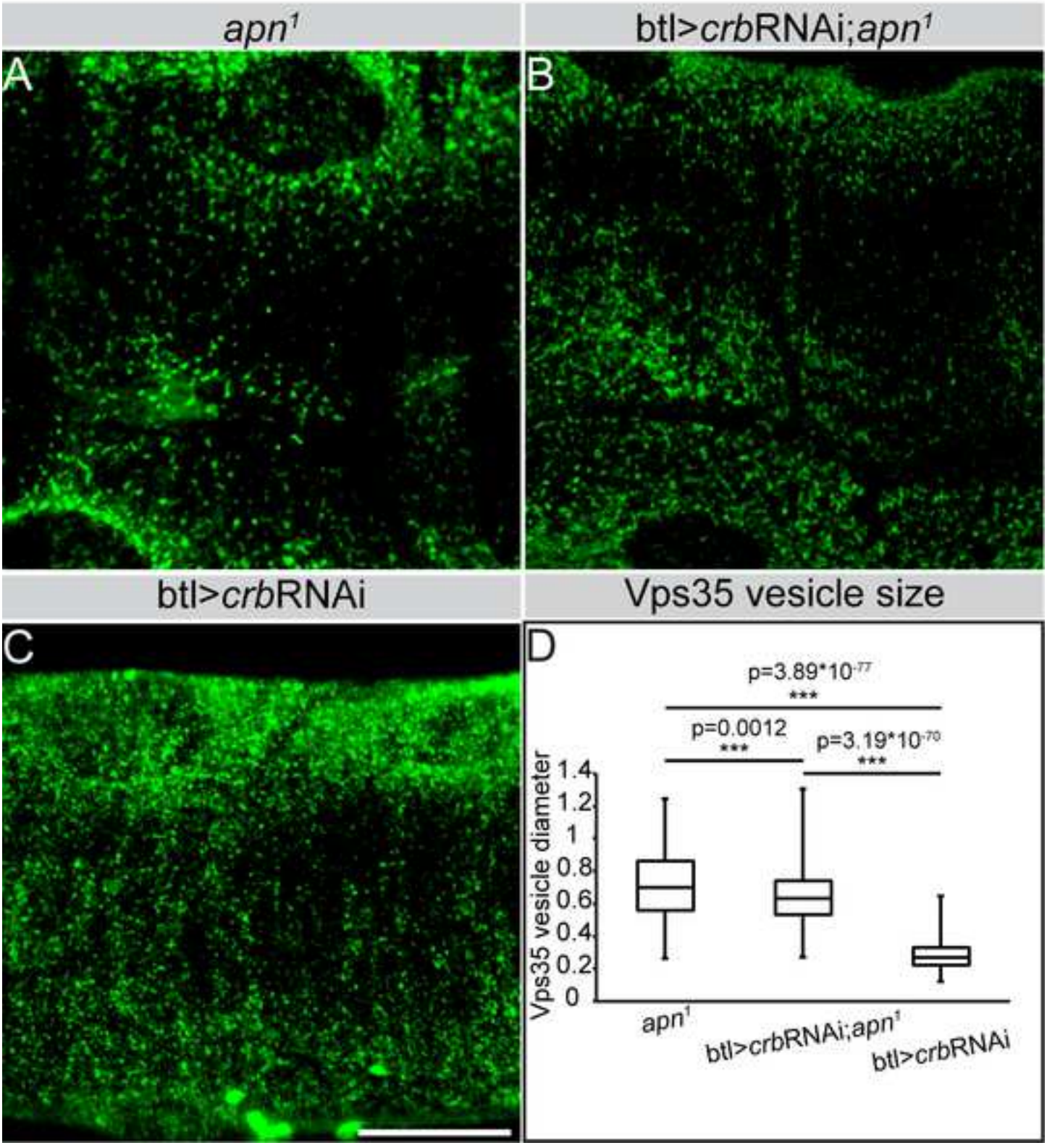

Figure 11

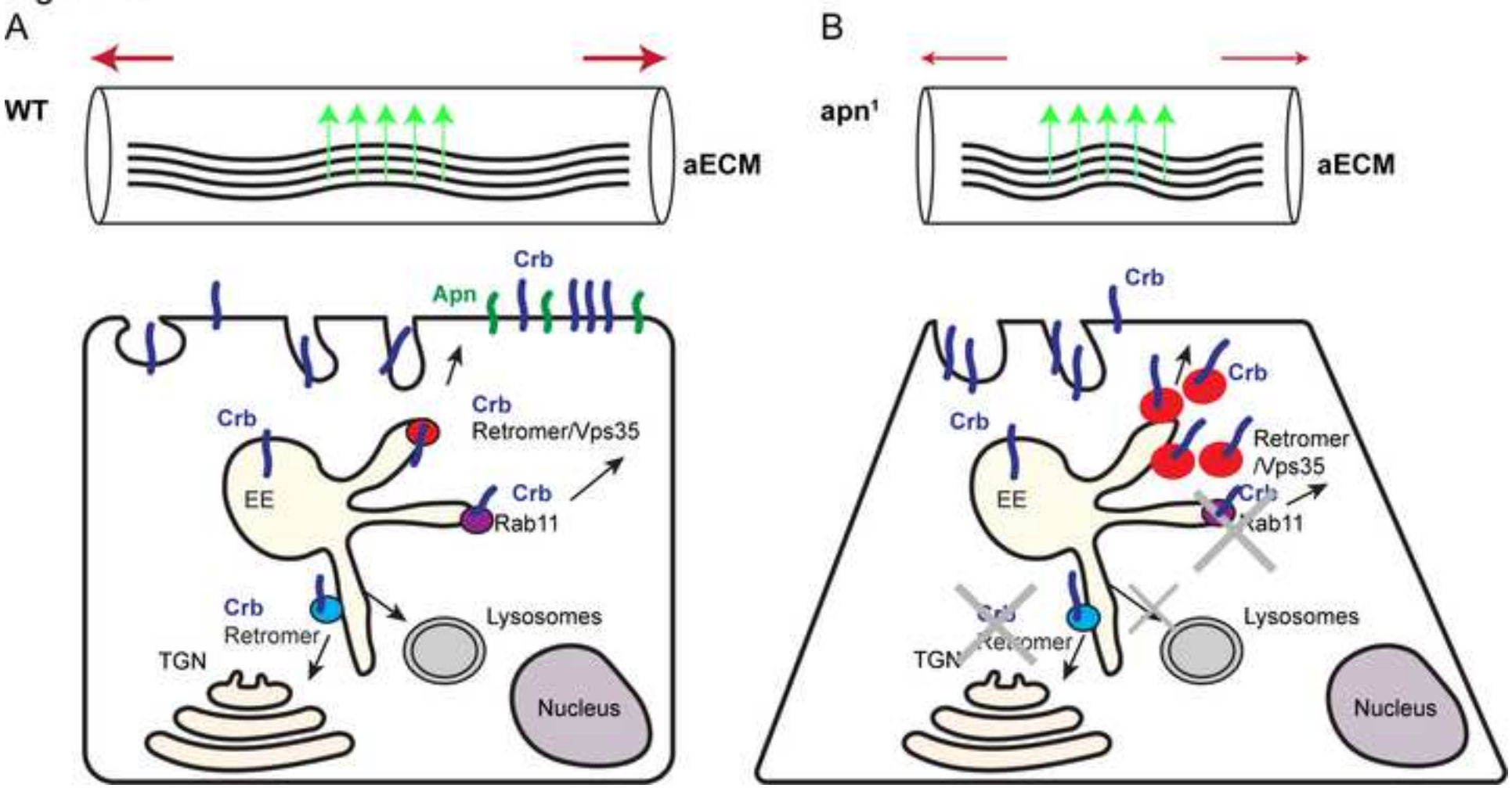

Suggested cover figure